reverse transcription-polymerase chain reaction (RT-PCR) and restriction fragment length polymorphism (RFLP) in the hemagglutinin-neuraminidase (HN) gene with *Sca*I and *Afl*II [12]. A simpler method was also reported through digestion with *Sca*I after DNA amplification by reverse transcription loop-mediated isothermal amplification (RT-LAMP) [13]. These methods are applied after immunization with the Hoshino vaccine. Now, two vaccine strains of the Torii and Hoshino are used, but no method of differentiation has been developed for the Torii strain. In this report, 584 nucleotides were amplified in the SH gene, and the two vaccine strains were distinguished from circulating wild types by unique restriction enzyme sites.

Materials and methods

Mumps virus and clinical samples

The Hoshino (Kitasato Institute, Tokyo, Japan) and Torii (Takeda Pharmaceutical, Osaka, Japan) vaccine strains were recovered from marketed vaccines. MuVi/Tokyo.JPN/77 (genotype B), MuVi/Akita.JPN/93-AK (genotype I), MuVi/Tokyo.JPN/94-H (genotype J), MuVi/Tokyo.JPN/94-0K (genotype B), and MuVi/Tokyo.JPN/01-III-10 (genotype L) were used as wild-type representatives for genotypes B, J, and L, which have already been reported [8–10]. A total of 47 clinical samples were examined: 20 cases of aseptic meningitis after immunization with the Torii strain, 25 cases after immunization with the Hoshino strain, and 2 cases of orchitis after immunization with the Hoshino strain. Two wild-type strains (MuVi/Tokyo.JPN/10-K and MuVi/Tokyo.JPN/10-F) were isolated and identified as genotype G. Cerebrospinal fluid (CSF) samples from the patients with aseptic meningitis and two salivary swab samples or nasopharyngeal swab (NPS) from the patients with orchitis were used.

RNA extraction

Total RNA was extracted from 200 μl CSF and salivary swabs or NPS using a magnetic bead RNA purification kit (MagExtractor-viral RNA; Toyobo, Osaka, Japan) and the RNA pellet was suspended in 30 μl distilled water.

RT-PCR and RLFP

RNA was transcribed to cDNA with a random hexamer using a PrimeScript RT reagent Kit (TaKaRa Bio, Japan) and amplified using Ex *Taq* DNA polymerase (TaKaRa Bio). The first PCR was done using MP F 921+ (5′TCTAT AATTCAATTGCCAGA) and MP HN241− (5′TGTCTGC AATTGAAGACAAC) and the nested PCR, using MpF0+ 5′GTCGATGATCTCATCAGGTAC) and Mp HN1− (5′C CAATATTCGGAAGCAGGTTCGGA), amplifying 584 nucleotides including the primer sequences from the genome positions 6139 to 6722 [10]. PCR products underwent electrophoresis after digestion with *Eco*T22I, *Mfe*I, and *Xba*I (New England BioLabs Japan).

Sequence analysis

PCR products were excised from low-melting gel electrophoresis and purified. DNA sequences were determined by the dye terminator method using an Applied Biosystems 3130 (Life Technologies Japan).

Results

Sequence analysis and restriction enzyme sites

The Hoshino and Torii strains were sequenced; alignments at the restriction enzyme sites are depicted in Fig. 1. The *Eco*T22I site (genome position 6386–6391) was unique to

	EcoT22 I	*Xba I*	*Mfe I*	*Mfe I*
	6386 6391	6437 6442	6451 6456	6589 6594
Torii [B]	ATGCAT	TCTAGA	CAGTTG	CAACTG
Hoshino [B]	-----G	------	--A---	T-----
JPN/77 [B]	-----G	------	---C--	-----C-
JPN/93AK [I]	-----G	------	-----A	---T--
JPN/94H [J]	-----G	------	--T--A	-----C-
JPN/94OK [B]	-----G	------	---C--	-----C-
JPN/01-III-10 [L]	-----A	------	-----T	------
JPN/10K [G]	-----G	-----G	-----A	---T--
JPN/10F [G]	-----G	-----G	-----A	---T--

Fig. 1 Sequence alignment of the Torii and Hoshino vaccine strains and representative wild strains. MuVi/Tokyo.JPN/77 (genotype B), MuVi/Akita.JPN/93-AK (genotype I), MuVi/Tokyo.JPN/94-H (genotype J), MuVi/Tokyo.JPN/94-0K (genotype B), and MuVi/Tokyo.JPN/01-III-10 (genotype L) were used. MuVi/Tokyo.JPN/10-K and MuVi/Tokyo.JPN/10-F (genotype G) are isolated in this study. Nucleotide changes are depicted in comparison with the Torii strain, and restriction enzyme sequences are highlighted in *grey*

Table 1 DNA sizes of restriction fragments after treatment with *Eco*T22I, *Mfe*I, and *Xba*I

Mumps strains	*Eco*T22I	*Mfe*I	*Xba*I
Hoshino genotype B	–	+ (313/271)	+ (299/285)
Torii genotype B	+ (332/252)	–	+ (299/285)
Wild genotypes B, J, L	–	–	+ (299/285)
Wild genotype I	–	+ (451/133)	+ (299/285)
Wild genotype G	–	+ (451/133)	–

the Torii strain and *Mfe*I site (6451–6456) to the Hoshino strain. Genotypes B, I, J, and L had an *Xba*I (6437–6442) site, and old genotype I and the currently circulating genotype G had an *Mfe*I site (6589–6594) newly introduced by nucleotide change, not at position 6451–6456 of the Hoshino strain. Based on the results of the sequence analysis, RFLP and predicted fragment lengths are shown in Table 1. The PCR product of the Hoshino strain was cut into two fragments (313 and 271) by *Mfe*I and that of the Torii strain into two fragments (332 and 252) by *Eco*T22I. These two strains were also cut by *Xba*I into two fragments (299 and 285). RFLP of the circulating wild type had mainly two patterns: genotypes B, J, and L were cut by *Xba*I and genotype G by *Mfe*I but differently from the Hoshino strain.

The results of RFLP are shown in Fig. 2. The PCR product of the Hoshino vaccine strain was cut by *Mfe*I and *Xba*I, and that of the Torii strain by *Eco*T22I and *Xba*I. As for the RFLP of wild type, the PCR product of MuVi/Akita.JPN/93-AK (genotype I) was cut by both *Mfe*I and *Xba*I with different fragment sizes from the Hoshino strain. MuVi/Tokyo.JPN/94-OK (genotype B) was cut by *Xba*I, and the same RFLP pattern was noted for MuVi/Tokyo.JPN/94-H (genotype J) and MuVi/Tokyo.JPN/01-III-10 (genotype L). PCR products of MuVi/Tokyo.JPN/10-K and/10-F (genotype G) were cut by *Mfe*I. They showed different patterns from the vaccine strains, as predicted from the sequencing results.

Differentiation of vaccine strains from wild types

A total of 47 clinical samples were obtained: 20 cases of aseptic meningitis after immunization with the Torii strain, 25 cases after immunization with the Hoshino strain, and 2 cases of orchitis after immunization with the Hoshino strain. The results of RT-PCR and RFLP are shown in Table 2. RT-PCR was negative for two CSF samples from the recipients of the Torii strain, and among 18 RT-PCR positives, 16 were identified as the Torii vaccine strain. Among 25 CSF samples obtained from the recipients of the Hoshino strain, 3 were negative by RT-PCR, and 20 were considered positive for the vaccine strain. Two from each

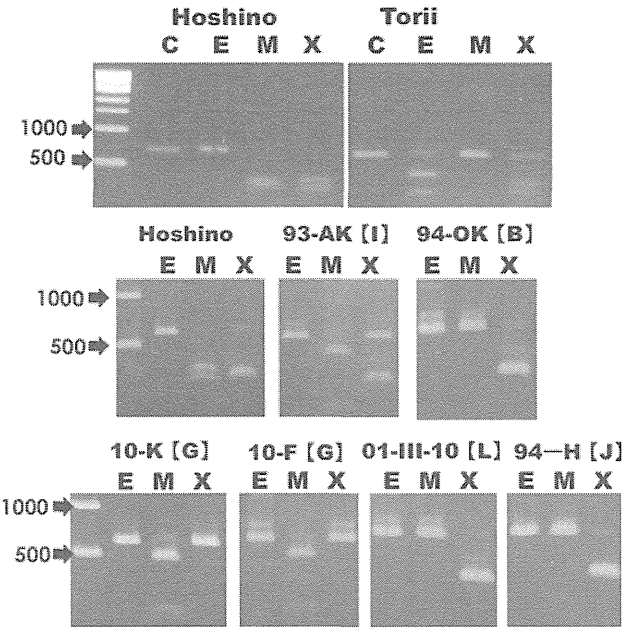

Fig. 2 Restriction fragment length polymorphism (RFLP) of the Hoshino and Torii vaccine strains and circulating wild strains. C, control; E, treatment with *Eco*T22I; M, treatment with *Mfe*I; X, treatment with *Xba*I. 93-AK, MuVi/Akita.JPN/93-AK [genotype I]; 94-H, MuVi/Tokyo.JPN/94-H [genotype J]; 94-OK, MuVi/Tokyo.JPN/94-0K [genotype B]; 01-III-10, MuVi/Tokyo.JPN/01-III-10 [genotype L]; 10-K, MuVi/Tokyo.JPN/10-K [genotype G]; 10-F, MuVi/Tokyo.JPN/10-F [genotype G]

were identified as wild strains. In 2 cases of orchitis after vaccination with the Hoshino strain, RT-PCR was positive in 1 case, identified as the wild type. Five of 45 patients with suspected adverse events were identified as having a concurrent wild-type genotype G.

Some strains identified as causing adverse events were sequenced; the phylogenetic analysis is shown in Fig. 3. Cases 1 and 2 were patients with aseptic meningitis after immunization with the Hoshino strain and cases A and B after that with the Torii strain. The sequencing results showed they were identical to the respective vaccine strains.

Table 2 Results of differentiation of mumps virus genome for clinical samples obtained from patients with aseptic meningitis and orchitis

	PCR negative	PCR positive	
		Vaccine strain	Wild strain
Aseptic meningitis after vaccination with			
Torii ($n = 20$)	2	16	2
Hoshino ($n = 25$)	3	20	2
Orchitis after vaccination with			
Hoshino ($n = 2$)	1		1

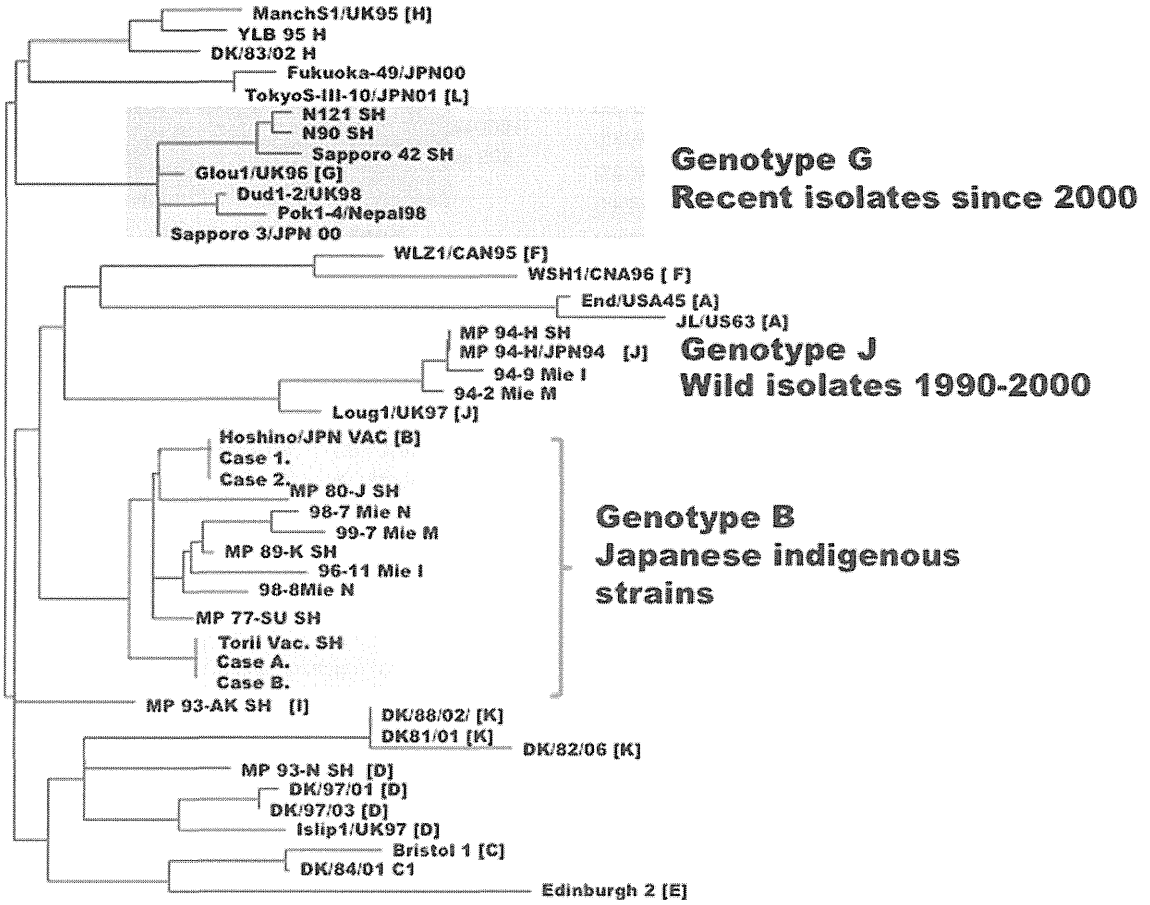

Fig. 3 Phylogenetic analysis of vaccine-associated cases in the small hydrophobic (SH) genome region. Cases 1 and 2 were patients with aseptic meningitis after immunization with the Hoshino strain and cases A and B after immunization with the Torii strain

Discussion

The mumps virus is classified into 12 distinct genotypes, with genotype B indigenous to Japan [4, 5, 8]. Genotype J was a dominant circulating strain with some genotype B strains in 1990–2000, and genotype G appeared in 2000–2012 with sporadic outbreaks of genotype L [8–10]. Mumps has been circulating in Japan because of a low immunization rate, approximately 30–40 %, and mump outbreaks have also been reported in the EU and USA where high immunization coverage was achieved with two doses of MMR [14–16]. The outbreaks were caused by the accumulation of susceptible individuals with an insufficient two-dose MMR vaccination in childhood. Several vaccine strains have been developed, and the Jeryl Lynn strain, belonging to genotype A, has been widely used as a component of MMR. Neutralization test (NT) antibody titers in sera obtained after vaccination with Jeryl Lynn were lower against genotype G than those against the vaccine strain, but they completely neutralized the other genotypes [17, 18]. In contrast, the antigenicity of genotype A of the vaccine strain was quite different from the recent circulating wild types and considered one of the reasons for the recirculation of the mumps virus [19]. There would be some problem with immunogenicity and persistence of immunity after immunization with the Jeryl Lynn strain. In Japan, two vaccine strains, Hoshino and Torii, are used and they belong to genotype B. In our previous report, there was no antigenic difference among circulating wild types [10]. Immunogenicity paralleled the incidence of adverse reactions. The incidence of aseptic meningitis after immunization with the Jeryl Lynn strain was reported to be 1 case in 100,000, and that of Torii or Hoshi was higher. The mump vaccine is still a voluntary one and so the cost is not covered by regional governments. Thus, guardians consider a mumps vaccination only when an outbreak is coming according to surveillance data. Some recipients were vaccinated by chance during the incubation period, and infection with the wild type became mixed into the vaccine-adverse events [12, 13]. In this report, 4 cases were identified as wild types among 45 cases with aseptic meningitis and 1 of the 2 cases of orchitis after immunization. From the results of surveillance reports, mumps outbreaks were observed in moderate grade, and

approximately 10 % of the vaccine-associated cases were infected with the wild type around the immunization day. Most adverse events developed 2–3 weeks after vaccination, but wild-type-related illness developed a few days earlier. There was no difference in clinical symptoms and clinical laboratory findings between vaccine-related adverse events and wild-type-related illness [3]. Five samples in aseptic meningitis and 1 in orchitis showed negative for mumps RT-PCR. Enterovirus RT-PCR for the mump PCR-negative samples showed negative for 5 mumps PCR-negative clinical samples [20]; these were considered to be low virus doses or in inappropriate stocking or transporting conditions.

Vaccine safety is a major concern and depends on postmarketing surveillance. Postmarketing surveillance from 1994 to 2010 is summarized, adding new data to the previous report [21], compared with the incidence of natural infections, in Table 3. The incidence of aseptic meningitis was <1–15 % among mumps infections with different incidences [22], and enhanced surveillance data showed 2.9 % of mumps patients were hospitalized, 6.1 % had orchitis, 0.3 % had meningitis, and 0.25 % had pancreatitis in England in 2002–2006 [23]. For the other complications, permanent deafness was considered to occur in approximately 1 per 20,000 cases, but it would actually be higher, 1 per 1,000 cases [24]. The results of postmarketing studies are shown from 1994 to 2010. A total of 3.5 million doses of the Hoshino vaccine were shipped, and acute parotitis was observed in 2–3 % of recipients. Among them, 117 nasopharyngeal swabs were examined and 89 were positive for RT-PCR: 64 were identified as the Hoshino vaccine strain and 25 were wild type. Among CNS complications, 5 cases of encephalopathy, 223 cases of aseptic meningitis, and 3 cases of acute disseminated encephalomyelitis (ADEM) were reported. Two cases were identified as enterovirus infections by RT-PCR [20]. When 85 CSF samples were examined in 223 cases of aseptic meningitis, 58 were considered vaccine-associated illnesses among 66 PCR positives. In this study period from 2008 to 2012, approximately 10 % of the patients suspected of having a vaccine-associated illness were identified as having wild-type infections during the mump outbreaks. Therefore, a simple differentiation method would contribute to further understanding of the safety of mumps vaccines.

Table 3 Complications of mumps and vaccine adverse events after vaccination with the Hoshino strain reported from 1994 to 2010

Complications	Natural infection	Vaccination (3.5 million)
Acute parotitis	70 %	2–3 %[a]
CNS complications		
Encephalopathy	1/5,000–6,000	5 (1: enterovirus)
Aseptic meningitis	1–2 %	223[b]
ADEM		3 (1: enterovirus)
Deafness	1/15,000 (1/1,000)	4
Orchitis	25 % in adolescents	15[c]
Oophoritis	5 %	
Pancreatitis	4 %	2
Other		1: ITP
		1: allergic purpura

Incidence of complications during natural infection refers to Ref. [22]

CNS, central nervous system; ADEM, acute disseminated encephalomyelitis; ITP, idiopathic thrombocytopenic purpura

[a] Of 117 nasopharyngeal swab (NPS) samples examined from patients with acute parotitis after vaccination with the Hoshino strain, PCR was positive in 89; 64 were identified as the vaccine strain and 25 as the wild type

[b] Of 85 CSF samples examined, 66 were PCR positive; 58 were identified as the vaccine strain and 8 as the wild type

[c] Three NPS samples were examined; one was the vaccine strain and two were the wild type

Conflict of interest The author has a conflict of interest. T.N. has received a research fund for the development of a new concept of live recombinant vaccines (20 million yen a year) from Daiichi-Sankyo Pharmaceutical.

References

1. Kimura M, Kuno-Sakai H, Yamazaki S. Adverse events associated with MMR vaccines in Japan. Acta Paediatr Jpn. 1996;38:205–11.
2. Ueda K, Miyazaki C, Hidaka Y, Okada K, Kusuhara K, Kadoya R. Aseptic meningitis caused by measles–mumps–rubella vaccine in Japan. Lancet. 1995;346:701–2.
3. Nagai T, Okafuji T, Miyazaki C, Ito Y, Kamada M, Kumagai T, et al. A comparative study of the incidence of aseptic meningitis in symptomatic natural mumps patients and monovalent mumps vaccine recipients in Japan. Vaccine. 2007;25:2742–7.
4. Jin L, Rima B, Brown D, Örvell C, Técle T, Afzal M, et al. Proposal for genetic characterization of wild-type mumps strains: preliminary standardisation of the nomenclature. Arch Virol. 2005;150:1903–9.
5. WHO. Mumps virus nomenclature update: 2012. A report based on the WHO mumps nomenclature update meeting, Geneva, 22 September 2011. Wkly Epidemiol Rec. 2012;87:217–24.
6. Sasaki K, Higashihara M, Inoue K, Igarashi Y. Studies on the development of a live attenuated mumps virus vaccine. Kitasato Arch Exp Med. 1976;49:43–52.
7. Hoshino M, Nishimitsu M, Ichimori Y, Oka Y, Kouno R, Yamashita K, et al. Development of live attenuated mumps Torii vaccine strain: development and biological characteristics. Clin Virol. 1981;9:323–30. (in Japanese).
8. Kashiwagi Y, Takami T, Mori T, Nakayama T. Sequence analysis of F, SH, and HN genes among mumps virus strains in Japan. Arch Virol. 1999;144:593–9.
9. Takahashi M, Nakayama T, Kashiwagi Y, Takami T, Sonoda S, Yamanaka T, et al. Single genotype of measles virus is dominant whereas several genotypes of mumps virus are co-circulating. J Med Virol. 1996;62:278–85.
10. Inou Y, Nakayama T, Yoshida N, Uejima H, Yuri K, Kamada M, et al. Molecular epidemiology of mumps virus in Japan and proposal of two new genotypes. J Med Virol. 2004;73:97–104.

11. Otto W, Mankertz A, Santibanez S, Saygilli H, Wenzel J, Jilg E, et al. Ongoing outbreak of mumps affecting adolescents and young adults in Bavaria, Germany, August to October 2010. Eur Surveill 2010;15(50):19748
12. Kashiwagi Y, Kawashima H, Takekuma K, Hoshika A, Mori T, Nakayama T. Detection of mumps virus genome directly from clinical samples and a simple method for genetic differentiation of the Hoshino vaccine strain from wild strains of mumps virus. J Med Virol. 1997;52:195–9.
13. Yoshida N, Fujino M, Ota Y, Notomi T, Nakayama T. Simple differentiation of mumps Hoshino vaccine strain from wild strains by reverse transcription loop-mediated isothermal amplification (RT-LAMP). Vaccine. 2007;25:1281–6.
14. CDC. Mumps epidemic—United Kingdom, 2004–2005. MMWR. 2006;55:173–5.
15. CDC. Mumps outbreak at a summer camp: New York, 2005. MMWR. 2006;55:175–7.
16. Barskey AE, Glasser J, LeBaron CW. Mumps resurgences in the United States: a historical perspective on unexpected elements. Vaccine. 2009;27:6186–95.
17. Rubin SA, Audet SA, Sullivan B, Carbone KM, Bellini WJ, Rota PA, et al. Antibody induced by immunization with Jeryl Lynn mumps vaccine strain effectively neutralizes a heterologous wild-type mumps virus associated with a large outbreak. J Infect Dis. 2008;198:508–15.
18. Rubin SA, Link MA, Sauder CJ, Zhang C, Ngo L, Rima BK, et al. Mumps outbreaks in vaccinated populations: no evidence of immune escape. J Virol. 2012;86:615–20.
19. Atrasheuskaya AV, Blatun EM, Kulak MV, Atrasheuskaya A, Karpov IA, Rubin S. Investigation of mumps vaccine failures in Minsk, Belarus, 2001–2003. Vaccine. 2007;25:4651–8.
20. Takami T, Kawashima H, Takei Y, Miyajima T, Mori T, Nakayama T, et al. Usefulness of nested PCR and sequence analysis in a nosocomial outbreak of neonatal enterovirus infection. J Clin Virol. 1998;11:67–75.
21. Nakayama T, Onoda K. Vaccine adverse events reported in post-marketing study of the Kitasato Institute from 1994–2004. Vaccine. 2007;25:570–6.
22. Plotkin SA, Rubin SA. Mumps vaccine. In: Plotkin SA, Orenstein W, Offit P, editors. Vaccines. 5th ed. Philadelphia: Saunders Elsevier; 2008. p. 435–65.
23. Yung CF, Andrews N, Bukasa A, Brown KE, Ramsay M. Mumps complications and effects of mumps vaccination, England and Wales, 2002–2006. Emerg Infect Dis. 2011;17:661–7.
24. Hashimoto H, Fujioka M, Kinumaki H, Kinki Ambulatory Pediatrics Study Group. An office-based prospective study of deafness in mumps. Pediatr Infect Dis J. 2009;28:173–5.

Microbiology and Immunology

Microbiol Immunol 2013; 57: 246–251
doi: 10.1111/1348-0421.12029

NOTE

Simple method for differentiating measles vaccine from wild-type strains using loop-mediated isothermal amplification

Tetsuo Nakayama[1], Akihito Sawada[1], Hideyuki Kubo[2], Atsushi Kaida[2], Toshimitsu Tanaka[3], Naoki Shigemoto[4], Katsuhiro Komase[5] and Makoto Takeda[5]

[1]Laboratory of Virus Infection, Kitasato Institute for Life Sciences, Shirokane 5-9-1, Minato-ku, Tokyo, 108-8641, Japan, [2]Osaka City Institute of Public Health and Environmental Sciences, Higashikamimachi 8-34, Tennouji-ku, Osaka, 543-0026, Japan, [3]Chiba City Institute of Public Health and Environmental Sciences, Saiwai-chou 1-3-9, Mihama-ku, Chiba, 261-0001, Japan, [4]Center for Public Health and Environment, Hiroshima Prefectural Technology Research Institute, Kaimi-chou 1-6-29, Minami-ku, Hiroshima, 734-007, Japan and [5]Department Virology III, National Institute for Infectious Diseases, Gakuen 4-7-1, Musashimurayama, Tokyo 208-0011, Japan

ABSTRACT

Because of increasing measles vaccine coverage, the proportion of patients with modified measles has been increasing. Such patients have low-grade fever with very mild eruptions similar to vaccine-related adverse events. Differentiation between these two pathogenic conditions is required to improve the quality of laboratory-based measles surveillance. In this study, vaccine-specific and wild-type specific primer sets were designed for loop-mediated isothermal amplification in the N gene, and vaccine strains, C1, D3, D4, D5, D8, D9, G3 and H1 wild strains were examined. Three vaccine strains were efficiently amplified using a vaccine-specific primer set with an approximately 10-times higher sensitivity than wild-type primer. Modified measles was differentiated from vaccine-associated cases by this system, but limitations were encountered with the other genotypes.

Key words LAMP, measles vaccine, modified measles.

Although the number of measles-related deaths decreased from 873,000 in 1999 to 164,000 in 2008, the goal set to reduce measles deaths by 2010 by 90% of those prior to 2000 was not achieved (1). Global single dose measles vaccination coverage increased from 72% in 2000 to 82% in 2007, when the two-dose immunization strategy was recommended for countries with high coverage (>95%) with the single dose measles vaccine. Most countries (88%) now implement the two-dose strategy (1). However, since late 2009, measles transmission has increased and outbreaks have become widespread in the European Union region because of failure to vaccinate susceptible populations (2). The World Health Assembly updated the goal of measles elimination to 95% reduction of 2000 figures for measles mortality by 2015 (3). In 2007–2008 in Japan, measles outbreaks with different characteristics occurred, namely most patients were young adults or adolescents attending high schools and universities in the early stages of the outbreak (4, 5). Because a relatively large proportion of those with adult measles had previously received single dose measles vaccination, they developed only mild grade fever and rash rather than typical measles symptoms (5). The patients with modified measles exhibited symptoms similar to the adverse events associated with vaccines, 10–20% of vaccine recipients developing low-grade fever (6). The diagnoses of modified measles were confirmed by virus isolation, detection of virus genome, or the serological responses of significant increase in IgG antibodies and/or presence of IgM antibodies (7).

Correspondence
Tetsuo Nakayama, Kitasato Institute for Life Sciences, Laboratory of Virus Infection, Shirokane 5-9-1, Minato-ku, Tokyo 108-8641, Japan.
Tel: +81 3 5791 6269; fax: +81 3 5791 6130; email: tetsuo-n@lisci.kitasato-u.ac.jp

Received 30 August 2012; revised 27 December 2012; accepted 7 January 2013.

List of Abbreviations: BIP, backward inner primer; FIP, forward inner primer; LAMP, loop-mediated isothermal amplification; RT-LAMP, reverse transcription loop-mediated isothermal amplification; vac-specific, vaccine-specific; wt-specific, wild type-specific.

However, using IgM positivity to diagnose modified measles in patients who have previously been vaccinated is not reliable. Virus isolation is not always successful because of issues like timing of sample collection, transport, low virus load, and short period of virus excretion in modified measles. The measles virus genome can be directly detected in clinical materials, and sequencing of the PCR products for molecular genotyping, targeting the N gene, would differentiate between adverse effects of vaccines and modified measles. However, this technique is time consuming and clinical samples do not contain sufficient amounts of viral RNA to perform sequencing analysis.

Circulating wild-type genotypes of measles virus are classified into 24 subclades. Of these, B1, C1, D1, E and F are considered inactive (8). In Japan, three measles vaccine strains have been used; the AIK-C and Schwarz FF8 strains, which have been further attenuated from the Edmonston strain, and CAM from the domestic wild-type, genotype A (9). It is critical to develop a simple method with high sensitivity and specificity for making an accurate diagnosis. Recent advances in molecular technology have improved the sensitivity and simplicity of genome amplification. A rapid diagnostic procedure for the detection of the measles genome using RT-LAMP has been reported (10, 11). In this study, that technique was modified for the discrimination of measles vaccine strain from wild circulating strains.

In Japan, C1, D3, D5 Palau-type, H1, D5 Bangkok-type and D9 have circulated since 1984 (5, 12). The following representative strains were used in this study: MVi/Tokyo.JPN/84-K [C1], MVi/Tokyo.JPN/37.99(Y) [D3], MVi/Tokyo.JPN/21.00 (O) [D5 Palau-type], MVi/Tokyo.JPN/20.00(S) [H1], MVi/Tokyo.JPN/17.07 [D5 Bangkok-type] and MVi/Aichi.JPN/44.06 [D9]. In 2011, D4, D8, D9 and G3 strains were imported from outside the country (National Institute of Infectious Diseases, Infectious Disease Surveillance Center; http://idsc.nih.go.jp/disease/measles/2011). MVi/Chiba C.JPN/08.11 [G3], MVi/Hiroshima.JPN/09.11 [D8] and MVi/Osaka C.JPN/09.11 [D4] were also investigated. During the measles outbreak in 2007–2008, 18 clinical samples were obtained from measles patients and those with non-typical measles characterized by mild febrile illness and eruptions (5). Of these, 13 stored samples were available for this study. Five vaccine-associated cases that occurred after 2008 were also investigated.

Total RNA was extracted from 200 μL of culture medium or clinical samples using a magnetic beads RNA purification kit (TOYOBO, Osaka, Japan) and re-suspended in 30 μL of distilled water. cDNA was synthesized from 5 μL of RNA, using a One Step PrimeScript RT-PCR Kit (TaKaRa Bio, Otsu, Japan) with poly T primer and random hexamer. Five microliters of cDNA was used for amplification of the measles genome by LAMP. The LAMP method was characterized by auto-cycling DNA synthesis using *Bst* DNA polymerase with strand displacement (New England BioLabs, Ipswich, MA, USA) and a specially designed set of primers, as is shown in Figure 1. Six LAMP primers were synthesized, recognizing eight different positions: of these F3, B3, F Loop, and BIP were the same as has previously been reported (11). In the present study, vaccine- and wild-type-specific FIPs and B Loop primers were used: vac-specific FIP (FIP-*Vac*: 5′-**TT**GTCCTCAGTAGTATG-CATTGCAGGTATCACTGCCGAGGATG), wt-specific FIP (FIP-*Wt*: 5′-**C**TGTCCTCAGTAGTATGCATTG-CAGGTATCACTGCCGAGGATG), vac-specific B loop (B Loop-*VAC*: 5′-TGAGAATGAGCTACC**GA**) and wt-specific B loop (B Loop-*Wt*: 5′-TGAGAATGAGCTAC-**CAG**) (Fig. 1). The bold letters at the 5′ end of the FIP and the 3′ end of the B loop are specific for the vaccine and wild-type sequences. The reaction mixture and procedure have previously been reported; differentiation between vaccine and wild-type strain was based on which primer set reached the threshold of LAMP amplification faster (11).

The N gene open reading frame of AIK-C and MVi/Tokyo.JPN/37.99(Y) [D3] were amplified and inserted into the multi-cloning sites of pBluescript SK II to construct pAIK-N and pWt D3-N. Serial dilutions of pAIK-N and pWt D3-N were subjected to vac-specific and wt-type specific LAMP; the results are shown in Figure 2. The detection limit of the measles AIK-C vaccine genome was 1–10 copies by vac-specific LAMP but 10–100 copies by wt-specific LAMP, indicating the latter is less efficient. Wild-type pWt D3-N was detected with a detection limit of 10–100 copies by wt-specific LAMP, more than 10 min faster than by vac-specific LAMP. This detection limit is similar to 30–100 copies achieved by the original RT-LAMP (11). The measles vaccine strain genomes from Schwarz FF-8 and CAM (10^4 TCID 50/mL) were amplified over 10 min faster using vac-specific LAMP than with wt-specific LAMP. The time differences between vac-specific and wt-specific LAMP in amplification increased with further dilutions.

Wild-type measles genotypes C1, D3, D4, D5 Palau, D5 Bangkok, D8, D9, G3 and H1 were also investigated. These isolates contained approximately 10^4 TCID 50/mL and serial 10-fold dilutions of cDNA were subjected to vac- and wt-specific LAMP. The results for the recent isolates D4, D5, D8, D9 and G3 are shown in Figure 3. The measles genome was efficiently amplified by wt-specific LAMP, more than 10 min earlier than by vac-specific LAMP in D4, D5 Palau, D5 Bangkok, D8 and D9 genotypes. As for the G3 isolate, 1:100 dilution of G3 was

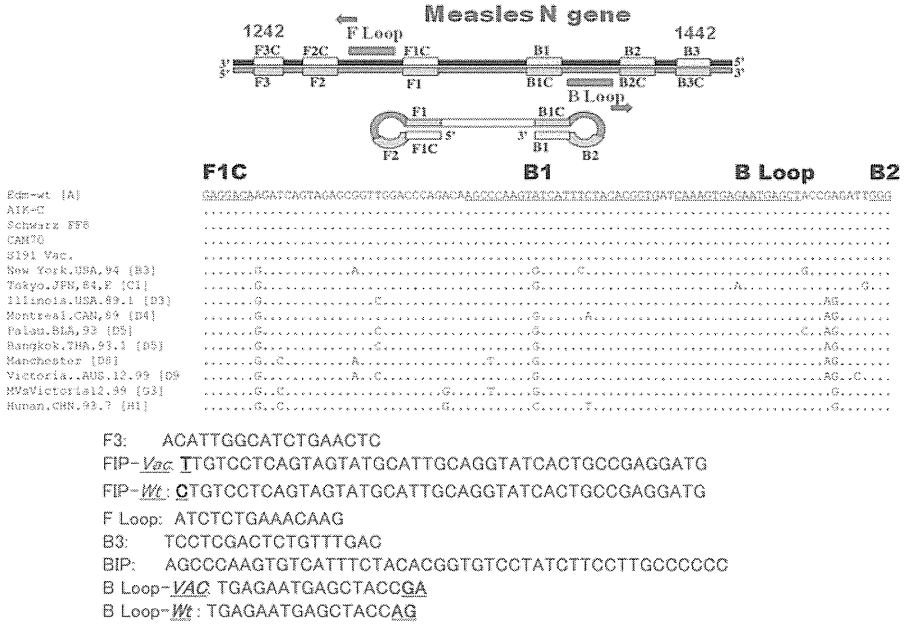

Fig. 1. Primer design for vaccine-specific and wild-type specific LAMP primers. The upper panel shows the location of LAMP primers schematically. The middle panel shows sequence alignments of vaccine and wild strains between F1C and B2 primer positions. Different nucleotides are depicted in comparison with the Edmonston and vaccine strains (AIK-C, Schwarz FF8, CAM70 and S191). The underlined sequence is the original measles LAMP primers. The lower panel shows the vac-specific and wt-specific LAMP primer sequences. The first bold letter at the 5′ end of FIP-*Vac* and FIP-*Wt* and the two bold letters at the 3′ end of B Loop-*Vac* and B Loop-*Wt* are specific to the indicated sequences.

amplified by wt-LAMP 3 min faster than by vac-LAMP and approximately 10 min faster for 1:1000 dilutions. The amplification profile of H1 was similar to that of G3. However, amplification times for C1 by vac-specific and wt-specific LAMP were within 1–2 min (data not shown).

Clinical samples obtained from the patients with low-grade fever and rash were examined; the results are shown in Figure 2. One had developed a febrile illness 10 days after immunization and the other during a measles outbreak, as previously reported (5). In the patient suspected of having an adverse event of vaccine, the measles genome was amplified only by the vac-specific LAMP, whereas the wild-type genome was amplified more efficiently by the wt-specific LAMP in the patient with modified measles during a measles outbreak. These two cases were confirmed by sequence analysis. Of the 13 stored samples from the 2007–2008 outbreak, all were efficiently amplified by wt-specific LAMP, as they had been by the original RT-LAMP. Of the five vaccine-associated cases after 2008, four were identified as vaccine strain. The remaining case was negative by both LAMP and RT-PCR. Conventional nested PCR and real-time PCR were also negative. This apparent discrepancy may have been caused by incorrect sample taking or transporting conditions.

After the World Health Organization in the Western Pacific Region set the goal of eliminating measles by 2012, a two dose schedule with a catch-up campaign for the forthcoming 5 years was implemented in Japan in 2008 (4). Thereafter, the number of reported cases of measles decreased from 11,015 in 2008 to 457 in 2010. Of 457 cases in 2010, approximately two-thirds were laboratory-confirmed, making the estimated incidence 3.58 per million. Some imported cases with D4, D8, D9 and H1 genotypes were reported (13). After the tsunami disaster in 2011, D4, D8, D9 and G3 strains were imported from outside the country (National Institute of Infectious Diseases, Infectious Disease Surveillance Center; http://idsc.nih.go.jp/disease/measles/2011pdf).

In the control phase, identification of the index case is difficult, especially for modified measles, because cross-reactivity with IgM measles antibody makes it hard to differentiate measles infection from rubella, parvovirus B19 infection and other virus infections (14). The proportion of modified measles cases with low-grade febrile illness and mild rash, similar to vaccine-associated illness is increasing. Restriction fragment length polymorphism was developed to differentiate between vaccine-associated adverse events and wild measles infection (15). The measles genome is amplified by RT-nested PCR, PCR products are electrophoresed after

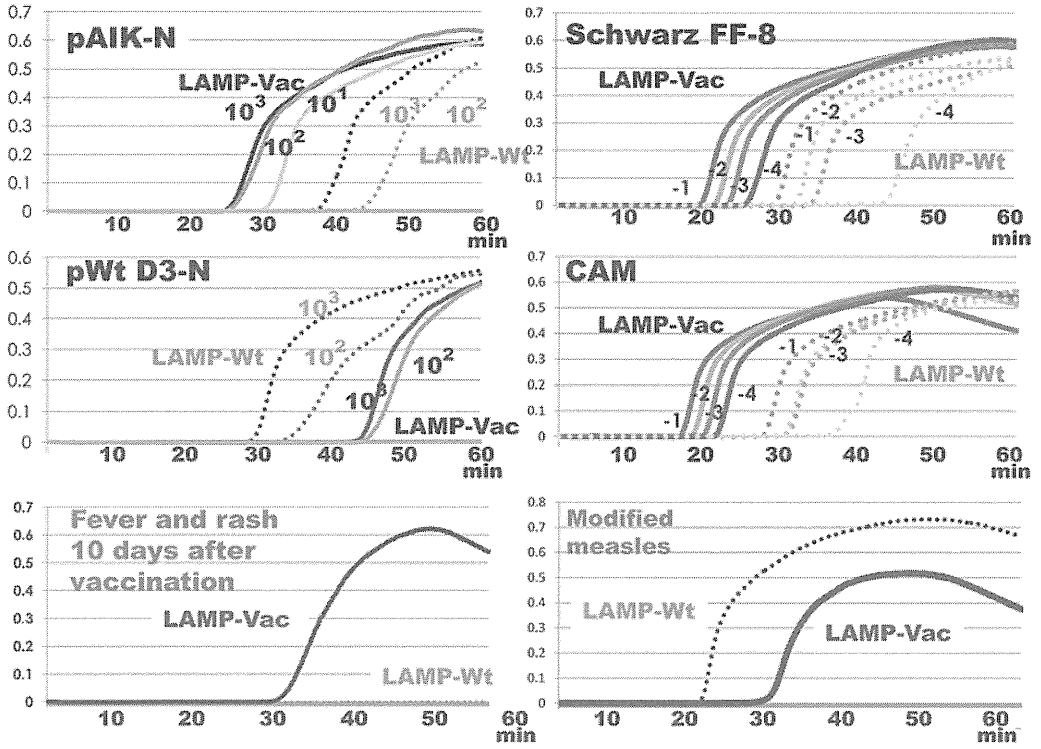

Fig. 2. Loop-mediated isothermal amplification (LAMP) reactions of the vaccine strains and comparison of their sensitivity. N gene expressing plasmids were constructed from AIK-C vaccine (pAIK-N) and D3 wild strain (pWt D3-N), plasmid concentrations were adjusted to 1000 copies/reaction and serial 10-fold dilutions pAIK-N and pWt D3-N were subjected to LAMP specific to the vaccine- and wild-type primer sets. The times to reach a threshold of 0.1 in turbidity (shown on the vertical axes) were compared. Dotted lines show amplification responses using the wild-type specific primer set and solid lines amplification responses using the vaccine-specific primer set. Results for two clinical samples are shown in the lower panels: the left panel from a patients suspected of having vaccine associated symptoms and the left from a patient with modified measles.
Wt, wild-type specific; Vac, vaccine-specific.

treatment with restriction enzymes; it takes several hours to obtain results.

Loop-mediated isothermal amplification amplifies target DNA with high sensitivity and specificity (10, 11). RT-LAMP systems reportedly detect several virus genomes with higher sensitivity than does conventional nested PCR. Mumps vaccine has the adverse effect of post-vaccination aseptic meningitis; a reported method for differentiating such reactions from infection involves digesting LAMP products with a specific restriction enzyme. Specifically, mumps Hoshino strain has a *Sca*I site in the LAMP target region and the LAMP-specific ladder pattern disappears after digestion with *Sca*I but does not do so with wild-type strains (16). This detection system requires additional procedures: opening the LAMP tube, treatment with the restriction enzyme and electrophoresis. Opening the LAMP tube is an undesirable operative step because it can lead to DNA cross-contamination. Single-step operations are ideal for obtaining accurate results. Because RSV has two distinctly different subgroups in the same target region, A and B, sequence-specific LAMP primers have been designed specifically for those subgroups; the subgroup-specific primer sets amplify their respective genomes (17).

The key reaction in LAMP is dumb-bell loop formation to react with FIP or BIP primers. The inner sequences of F1 and B1 are critical for such loop construction (10). The FIP primer consists of 5′ F1 complement connected to the F2 sequence, and the 5′ end of FIP or BIP is critical for binding to the 3′ portion of F1 or B1. In a previous study, LAMP primers were designed in the conserved regions to detect the measles genome with high sensitivity. Sequence results for the F1 and B1 of vaccine and wild-type strains have shown that all vaccine strains have A at genome position 1321, whereas all wild-types have G in this position (11). In the present study, vaccine-specific and wild-type-specific FIP primers were designed to have one nucleotide shift to the inner region in comparison with the previous original LAMP FIP primer sequence, which adds T at the 5′ end of FIP for vaccine-specific and C for wild-type-specific FIP. The addition of loop primers results in a shorter reaction time

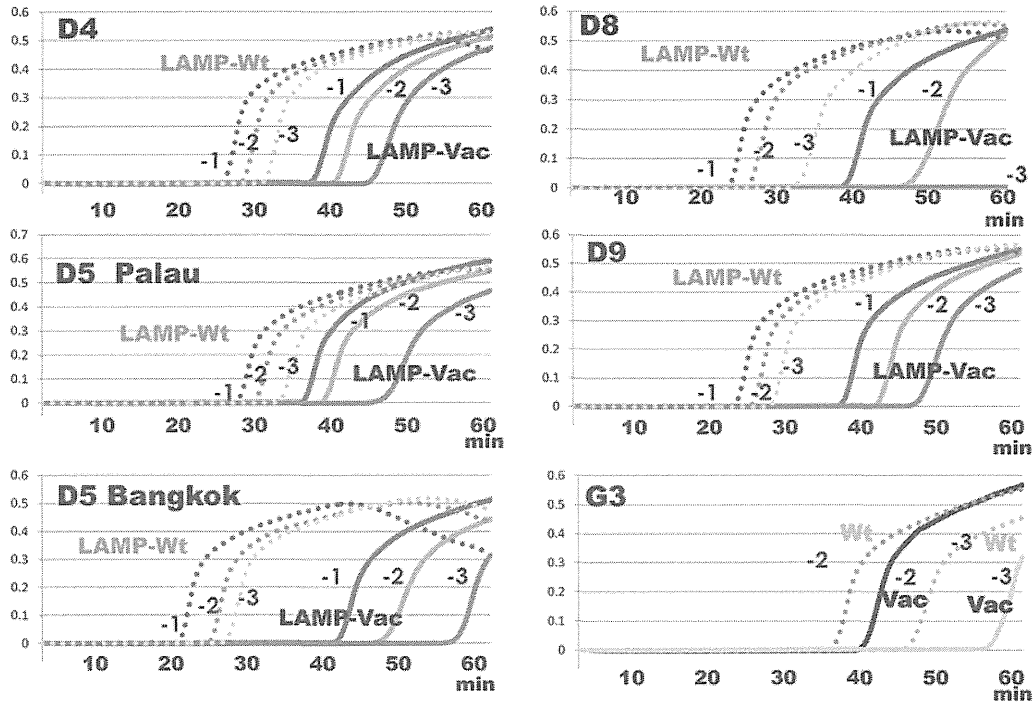

Fig. 3. Loop-mediated isothermal amplification (LAMP) reactions of wild types, D4, D5, D8, D9 and G3. RNA of virus isolates was converted to cDNA and serial 10-fold dilutions subjected to LAMP reaction. The times to reach a threshold of 0.1 in turbidity were compared. Dotted lines show amplification responses using wild-type specific primer set and solid lines by vaccine-specific primer set.
LAMP-Wt, wild-type specific primer set; LAMP-Vac, vaccine-specific primer set.

for displacement of the stem loop region and most genotypes have GG or AG (genome positions 1397 and 1398) at the 3′ end of B Loop primer. All wild-types, except the C1 strain, were amplified more efficiently by wt-specific LAMP than by vac-specific LAMP. However, the difference in amplification time for C1 with vac-specific and wt-specific LAMP was within 1–2 min. Because B2, B3, and C2 have the same sequences at the 5′ end of FIP and the 3′ end of B loop to the C1 genotype, their ability to discriminate would be similar. C1 genotype is inactive. So far, B2, B3 and C2 genotypes have not been introduced into Japan, but are still active (8, 12, 13). There would be a possibility of invasion. When there is no definite amplification delay, sequence analysis should be performed. As for G3 and H1, the time difference in genome amplification by wt-specific and vac-specific LAMP became apparent in samples with lower genome concentrations.

Among five clinical samples obtained from the patients suspected vaccine-associated adverse events, four were confirmed as vaccine adverse events, demonstrating the genome-amplification by vaccine specific primer set. In Japan, C1, D3, D5 Palau-type, H1, D5 Bangkok-type and D9 have circulated since 1984 (5, 12, 13), and D4, D8, D9 and G3 strains were imported from outside the country in 2011 (National Institute of Infectious Diseases, Infectious Disease Surveillance Center; http://idsc.nih.go.jp/disease/measles/2011). Clinical samples of D4, D8, D9 and G3 were not obtained but the differentiation method using vac- and wt-specific LAMPs would work for surveillance study.

DISCLOSURE

All authors have no conflicts of interest regarding this study.

REFERENCES

1. WHO. (2009) Measles vaccines: WHO position paper. *Wkly Epidemiol Rec* **84**: 349–60.
2. CDC. (2011) Increased transmission and outbreaks of measles—European region, 2011. *MMWR* **60**: 1605–10.
3. Okwo-Bele J.M., Cherian T. (2011) The expanded programme on immunization: a lasting legacy of smallpox eradication. *Vaccine* **29S**: D74–79.
4. CDC. (2008) Progress toward measles elimination—Japan, 1999-2008. *Morbidity and Mortality Weekly Report* **57**: 1049–52.
5. Nagai M., Ji Y-X., Yoshida N., Miyata A., Fujino M., Ihara T., Yoshikawa T., Asano Y., Nakayama T. (2009) Modified adult

measles in outbreaks in Japan, 2007- 2008. *J Med Virol* **81**: 1094–101.
6. Makino S. (1983) Development and characteristics of live AIK-C measles virus vaccine: a brief report. *Rev Infect Dis* **5**: 504–5.
7. WHO. (2005) Global measles and rubella laboratory network—update. *Wkly Epidemiol Rec* **80**: 384–8.
8. WHO. (2012) Measles virus nomenclature update: 2012. *Wkly Epidemiol Rec* **87**: 73–81.
9. Hirayama M. (1983) Measles vaccines used in Japan. *Rev Infect Dis* **5**: 495–503.
10. Notomi T., Okayama H., Masubuchi H., Yonekawa T., Watanabe K., Amino N., Hase T. (2000) Loop-mediated isothermal amplification of DNA. *Nucleic Acids Res* **28**: e63.
11. Fujino M., Yoshida N., Yamaguchi S., Hosaka N., Ota Y., Notomi T., Nakayama T. (2005) A simple method for the detection of measles virus genome by loop-mediated isothermal amplification (LAMP). *J Med Virol* **76**: 406–13.
12. Nakayama T., Fujino M., Yoshida N. (2004) Molecular epidemiology of measles virus in Japan. *Pediatr Int* **46**: 214–21.
13. National Institute of Infectious Diseases of Japan, Infectious Diseases Surveillance Center. (2011) Measles in 2010. *Infectious Agents Surveillance Report* **32**: 31–32.
14. Thomas H.I.J., Barrett E., Hesketh L.M., Wynne A., Morgan-Carpner P. (1999) Simultaneous IgM reactivity by EIA against more than one virus in measles, parvovirus B19 and rubella infection. *J Clin Virol* **14**: 107–18.
15. Mori T. (1994) A simple method for genetic differentiation of the AIK-C vaccine strain from wild strains of measles virus. *Biologicals* **22**: 179–85.
16. Yoshida N., Fujino M., Ota Y., Notomi T., Nakayama T. (2007) Simple differentiation method of mumps Hoshino vaccine strain from wild strains by reverse transcription loop-mediated isothermal amplification (RT-LAMP). *Vaccine* **25**: 1281–6.
17. Ushio M., Yui I., Yoshida N., Fujino M., Yonekawa T., Ota Y., Notomi T., Nakayama T. (2005) Detection of respiratory syncytial virus genome by subgroups-A, B specific reverse transcription loop-mediated isothermal amplification (RT-LAMP). *J Med Virol* **77**: 121–7.

LETTER

doi:10.1038/nature12392

Characterization of H7N9 influenza A viruses isolated from humans

Tokiko Watanabe[1]*, Maki Kiso[2]*, Satoshi Fukuyama[1]*, Noriko Nakajima[3]*, Masaki Imai[4]*, Shinya Yamada[2], Shin Murakami[5], Seiya Yamayoshi[2], Kiyoko Iwatsuki-Horimoto[2], Yoshihiro Sakoda[6], Emi Takashita[4], Ryan McBride[7], Takeshi Noda[2], Masato Hatta[8], Hirotaka Imai[8], Dongming Zhao[1], Noriko Kishida[4], Masayuki Shirakura[4], Robert P. de Vries[7], Shintaro Shichinohe[6], Masatoshi Okamatsu[6], Tomokazu Tamura[6], Yuriko Tomita[1], Naomi Fujimoto[1], Kazue Goto[1], Hiroaki Katsura[2], Eiryo Kawakami[1], Izumi Ishikawa[1], Shinji Watanabe[1,9], Mutsumi Ito[2], Yuko Sakai-Tagawa[2], Yukihiko Sugita[2], Ryuta Uraki[2], Reina Yamaji[2], Amie J. Eisfeld[8], Gongxun Zhong[8], Shufang Fan[8], Jihui Ping[8], Eileen A. Maher[8], Anthony Hanson[8], Yuko Uchida[10], Takehiko Saito[10], Makoto Ozawa[11,12], Gabriele Neumann[8], Hiroshi Kida[6,13], Takato Odagiri[4], James C. Paulson[7], Hideki Hasegawa[3], Masato Tashiro[4] & Yoshihiro Kawaoka[1,2,5,8,14]

Avian influenza A viruses rarely infect humans; however, when human infection and subsequent human-to-human transmission occurs, worldwide outbreaks (pandemics) can result. The recent sporadic infections of humans in China with a previously unrecognized avian influenza A virus of the H7N9 subtype (A(H7N9)) have caused concern owing to the appreciable case fatality rate associated with these infections (more than 25%), potential instances of human-to-human transmission[1], and the lack of pre-existing immunity among humans to viruses of this subtype. Here we characterize two early human A(H7N9) isolates, A/Anhui/1/2013 (H7N9) and A/Shanghai/1/2013 (H7N9); hereafter referred to as Anhui/1 and Shanghai/1, respectively. In mice, Anhui/1 and Shanghai/1 were more pathogenic than a control avian H7N9 virus (A/duck/Gunma/466/2011 (H7N9); Dk/GM466) and a representative pandemic 2009 H1N1 virus (A/California/4/2009 (H1N1pdm09); CA04). Anhui/1, Shanghai/1 and Dk/GM466 replicated well in the nasal turbinates of ferrets. In nonhuman primates, Anhui/1 and Dk/GM466 replicated efficiently in the upper and lower respiratory tracts, whereas the replicative ability of conventional human influenza viruses is typically restricted to the upper respiratory tract of infected primates. By contrast, Anhui/1 did not replicate well in miniature pigs after intranasal inoculation. Critically, Anhui/1 transmitted through respiratory droplets in one of three pairs of ferrets. Glycan arrays showed that Anhui/1, Shanghai/1 and A/Hangzhou/1/2013 (H7N9) (a third human A(H7N9) virus tested in this assay) bind to human virus-type receptors, a property that may be critical for virus transmissibility in ferrets. Anhui/1 was found to be less sensitive in mice to neuraminidase inhibitors than a pandemic H1N1 2009 virus, although both viruses were equally susceptible to an experimental antiviral polymerase inhibitor. The robust replicative ability in mice, ferrets and nonhuman primates and the limited transmissibility in ferrets of Anhui/1 suggest that A(H7N9) viruses have pandemic potential.

Influenza A virus infections place a considerable burden on public health and the world economy. In March 2013, several individuals were reported to be infected with an avian A(H7N9) virus[1,2]. Viruses of this subtype do not circulate in humans, so A(H7N9) viruses capable of transmitting among humans would encounter populations that lack any protective immunity to them. By May 30 2013, 132 confirmed human infections with A(H7N9) viruses had been reported, with 37 deaths[3], resulting in a case fatality rate of >25%.

Sequence and phylogenetic analysis revealed that the haemagglutinin (HA) and neuraminidase (NA) genes of the A(H7N9) viruses originated from avian H7 and N9 viruses, respectively[2,4,5], whereas the remaining six genes are closely related to H9N2 subtype viruses that have circulated in poultry in China[2,4,5]. Several of the A(H7N9) viruses possess amino acid changes known to facilitate infection of mammals, such as leucine at position 226 of HA (H3 HA numbering), which confers increased binding to human-type receptors[6], and the mammalian-adapting mutations E627K[7,8] or D701N[9] in the PB2 polymerase subunit. Notably, the PB2-627K or PB2-701N markers have been detected in almost all human, but not avian or environmental, A(H7N9) isolates, suggesting ready adaptation of A(H7N9) viruses to humans.

To characterize the biological properties and pandemic potential of A(H7N9) viruses, we compared Anhui/1 (which possesses the mammalian-adapting HA-226L and PB2-627K markers) and Shanghai/1 (which possesses the 'avian-type' HA-226Q and mammalian-adapting PB2-627K markers) with the phylogenetically unrelated avian H7N9 Dk/GM466 virus, and with CA04, an early, representative 2009 H1N1 pandemic virus. Anhui/1, Shanghai/1 and CA04 replicated efficiently in Madin–Darby canine kidney (MDCK) cells and in differentiated normal human bronchial epithelial cells compared with Dk/GM466, especially at 33 °C, a temperature corresponding to the human upper airway (Supplementary Fig. 1). Electron microscopic analysis showed Anhui/1 as a spherical particle that appeared to be efficiently released from infected cells (Supplementary Fig. 2).

Next, we assessed the pathogenicity of Anhui/1 and Shanghai/1 in established animal models in influenza virus research, namely mice, ferrets and nonhuman primates (Anhui/1 only). In BALB/c mice, Anhui/1 and Shanghai/1 were more pathogenic than CA04 and Dk/GM466 on the basis of MLD_{50} (mouse lethal dose 50; the dose required to kill 50% of infected mice) values, which were $10^{3.5}$ plaque-forming units (p.f.u.) for Anhui/1 and Shanghai/1, $10^{5.5}$ p.f.u. for CA04 and $10^{6.7}$ p.f.u. for Dk/GM466 (Supplementary Fig. 3). Three days post-infection

[1]ERATO Infection-Induced Host Responses Project, Japan Science and Technology Agency, Saitama 332-0012, Japan. [2]Division of Virology, Department of Microbiology and Immunology, Institute of Medical Science, University of Tokyo, Tokyo 108-8639, Japan. [3]Department of Pathology, National Institute of Infectious Diseases, Shinjuku, Tokyo 162-8640, Japan. [4]Influenza Virus Research Center, National Institute of Infectious Diseases, Musashimurayama, Tokyo 208-0011, Japan. [5]Department of Special Pathogens, International Research Center for Infectious Diseases, Institute of Medical Science, University of Tokyo, Minato-ku, Tokyo 108-8639, Japan. [6]Laboratory of Microbiology, Department of Disease Control, Graduate School of Veterinary Medicine, Hokkaido University, Sapporo 060-0818, Japan. [7]The Scripps Research Institute, 10550 North Torrey Pines Road, SP-3 La Jolla, California 92037, USA. [8]Department of Pathobiological Sciences, School of Veterinary Medicine, University of Wisconsin-Madison, 575 Science Drive, Madison, Wisconsin 53711, USA. [9]Laboratory of Veterinary Microbiology, Department of Veterinary Sciences, University of Miyazaki, Miyazaki 889-2192, Japan. [10]Influenza and Prion Disease Research Center, National Institute of Animal Health, Kannondai 3-1-5, Tsukuba, Ibaraki 305-0856, Japan. [11]Laboratory of Animal Hygiene, Joint Faculty of Veterinary Medicine, Kagoshima University, Kagoshima 890-0065, Japan. [12]Transboundary Animal Disease Center, Joint Faculty of Veterinary Medicine, Kagoshima University, Kagoshima 890-0065, Japan. [13]Research Center for Zoonosis Control, Hokkaido University, Sapporo 001-0020, Japan. [14]Laboratory of Bioresponses Regulation, Department of Biological Responses, Institute for Virus Research, Kyoto University, Kyoto 606-8507, Japan.
*These authors contributed equally to this work.

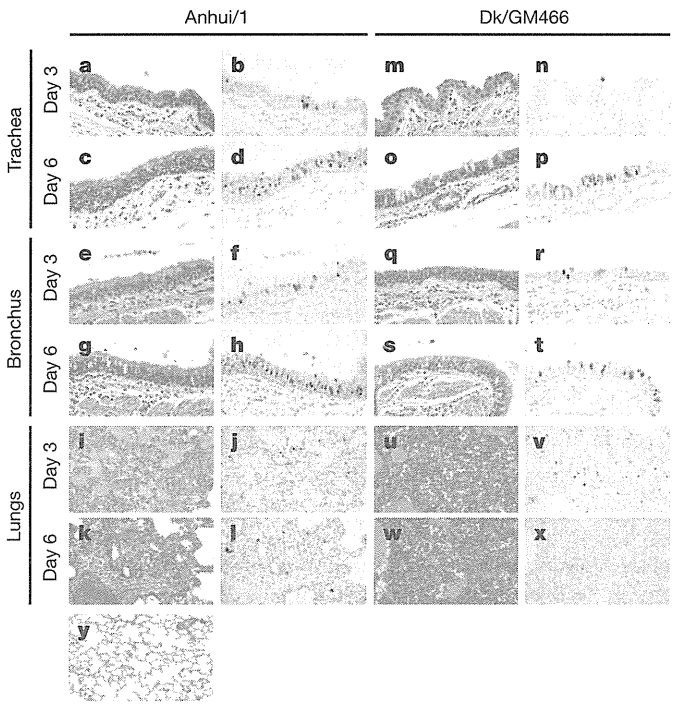

Figure 1 | Pathological findings in infected macaques. **a–x**, Shown are pathological findings in the trachea (**a–d, m–p**), bronchus (**e–h, q–t**) and lungs (**i–l, u–x**) of macaques infected with Anhui/1 (**a–l**) or Dk/GM466 (**m–x**) at 3 d.p.i. (**a, b, e, f, i, j, m, n, q, r, u, v**) or 6 d.p.i. (**c, d, g, h, k, l, o, p, s, t, w, x**), with haematoxylin and eosin staining (**a, c, e, g, i, k, m, o, q, s, u, w**) or immunohistochemistry for influenza viral antigen (**b, d, f, h, j, l, n, p, r, t, v, x**). **y**, Haematoxylin and eosin staining of the lung of an uninfected macaque is shown. Original magnifications: ×400 (**a–h, m–t**), ×200 (**i–l, u–y**).

(d.p.i.), virus titres in the lungs and nasal turbinates of Anhui/1-, Shanghai/1- and CA04-infected mice were slightly higher than those in Dk/GM466-infected mice (Supplementary Table 1). Lung lesions in Anhui/1- and CA04-infected mice were more severe than those in Dk/GM466-infected mice, in particular at 6 d.p.i. (Supplementary Fig. 4). Bronchitis, bronchiolitis, thickening of the alveolar septa, oedema and interstitial inflammatory cell infiltration were also more prominent in Anhui/1- and CA04-infected mice. Viral antigen was detected in many alveolar and bronchial epithelial cells at 3 d.p.i. in Anhui/1- and CA04-infected mice (Supplementary Fig. 4), whereas viral-antigen-positive cells were restricted to a few bronchial epithelial cells in Dk/GM466-infected mice (Supplementary Fig. 4). Collectively, these findings demonstrate that Anhui/1 is as pathogenic as CA04 and more pathogenic than Dk/GM466 in mice.

Ferrets intranasally infected with Anhui/1, Shanghai/1, CA04 or Dk/GM466 experienced loss of appetite. Transient weight loss was detected in one of the three animals infected with Anhui/1 (Supplementary Fig. 5). Virus titres in the trachea of Anhui/1-, Shanghai/1- and CA04-infected ferrets were higher at 3 d.p.i. than those obtained from Dk/GM466-infected animals (Supplementary Table 2); at 6 d.p.i., virus was isolated from the trachea of Anhui/1-, Shanghai/1- and Dk/GM466-infected animals, but not from that of CA04-infected ferrets. All three viruses replicated inefficiently in the lungs of these animals. In this study, we did not detect virus in the lungs in the CA04-infected animals at 3 d.p.i. (Supplementary Table 2), whereas this virus was recovered from two out of three ferrets infected at 3 d.p.i. in our previous study[10], consistent with efficient replication of pandemic 2009 H1N1 virus in the lungs of ferrets as reported by others[11–14]. Appreciable amounts of virus were recovered from nasal turbinates at 3 and 6 d.p.i., with the exception of the nasal turbinates of CA04-infected animals at 6 d.p.i. (Supplementary Table 2). Inflammation was prominent in the trachea and submucosal glands of CA04-infected ferrets (Supplementary Fig. 6). Viral-antigen-positive cells were detected in the tracheal, glandular and alveolar epithelial cells of all ferrets. Anhui/1- and CA04-infected ferrets displayed numerous viral-antigen-positive cells, especially in the glandular epithelia, whereas Dk/GM466-infected ferrets presented far fewer antigen-positive cells. Viral antigens were also detected in pneumocytes in localized lung lesions of each ferret. In mediastinal lymph nodes, viral antigen was detected in Anhui/1- and CA04-infected ferrets only. Anhui/1 and Shanghai/1 thus established a robust, although relatively mild, infection in the upper respiratory organs of ferrets that was unlike most avian H5N1 influenza virus infections in ferrets, which consistently cause severe symptoms including profound weight loss.

Infection of cynomolgus macaques (*Macaca fascicularis*) with 6.7×10^7 p.f.u. of Anhui/1 or Dk/GM466 caused fever (Supplementary Fig. 7), as did infection with CA04 in our previous study[10]. Both Anhui/1 and Dk/GM466 replicated appreciably in macaque nasal turbinates, trachea and lungs, although variability among the virus titres was noticed, as is commonly found among outbred animals (Supplementary Tables 3 and 4a). Previously, we detected efficient replication of CA04 in the respiratory organs of cynomolgus macaques at 3 d.p.i.; by 7 d.p.i., no virus was detected in the lungs[10].

Pathological examination of the respiratory organs did not reveal major differences between macaques infected with Anhui/1 or Dk/GM466; no notable lesions were detected in the trachea or lobular bronchus, but alveolar spaces contained oedematous exudate and inflammatory infiltrates comprising mainly neutrophils and monocytes/macrophages (Fig. 1). At 6 d.p.i., regenerative changes were observed. Lung inflammation scores did not reveal appreciable differences between animals infected with Anhui/1 or Dk/GM466 (Supplementary Table 4b). Numerous tracheal and bronchial epithelial cells of Anhui/1-infected macaques were positive for viral antigen (Fig. 1b, d, f, h), as was observed in our previous study with CA04 at 7 d.p.i.[10]. Fewer antigen-positive cells in the tracheal and bronchial epithelia of Dk/GM466-infected animals were detected, in particular

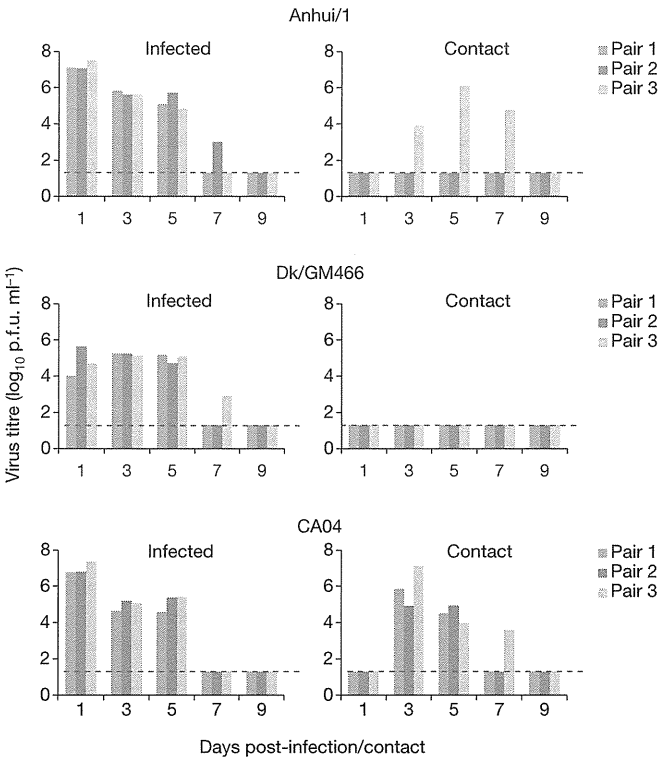

Figure 2 | Respiratory droplet transmission in ferrets. Ferrets were infected with 5×10^5 p.f.u. of Anhui/1, Dk/GM466 or CA04 (infected ferrets). One day later, three naive ferrets (contact ferrets) were each placed in a cage adjacent to an infected ferret. Nasal washes were collected from infected ferrets on day 1 after inoculation and from contact ferrets on day 1 after co-housing, and then every other day (up to 9 days) for virus titration.

at 3 d.p.i. (Fig. 1n, r). Viral antigen was also detected in the mediastinal lymph node sections of Anhui/1-infected monkeys (Supplementary Fig. 8). In addition, our analysis of chemokine/cytokine responses suggests that Anhui/1 induces strong inflammatory responses both systemically and at the site of virus infection (Supplementary Fig. 9 and Supplementary Information).

No sustained human-to-human transmission of the novel A(H7N9) viruses has been reported to date. To assess the transmissibility of Anhui/1, naive 'contact' ferrets in wireframe cages (which prevent direct contact with animals in neighbouring cages, but allow respiratory droplet transmission) were placed adjacent to an 'infected' ferret the day after infection as described previously[15]. We recovered viruses from the nasal washes of all three contact ferrets for CA04 (Fig. 2), as expected on the basis of previous studies by us[10] and others[13,14]. No virus was detected in the nasal washes of contact ferrets for Dk/GM466 (Fig. 2), consistent with the general lack of transmissibility of avian influenza viruses in ferrets. However, one of three contact ferrets for Anhui/1 shed virus on days 3–7 after contact (Fig. 2). Serum antibody titres against Anhui/1 confirmed infection of this animal, whereas the other two contact animals did not seroconvert (Supplementary Table 5). Given that avian H5N1 influenza viruses require several mutations to transmit through respiratory droplets among ferrets[15–18], the pandemic potential of A(H7N9) viruses may be greater than that of the highly pathogenic avian H5N1 influenza viruses.

Because replication and transmission of an H5 HA-possessing virus in ferrets is associated with amino acid changes in HA[15,18], we sequenced the genomes of viruses obtained from infected and contact ferrets. Compared to virus inoculum, we detected three non-synonymous mutations in HA (T71I, R131K and A135T; Fig. 3 and Supplementary Table 6) and one nonsynonymous mutation in NA (A27T; N9 numbering) (Supplementary Table 6); we also detected several synonymous nucleotide changes. The amino acid mutations in HA were detected in >40% of the molecular clones derived from samples obtained on day 3 post-contact (Supplementary Table 7), but were found exclusively by day 5 post-contact. Interestingly, the egg-grown virus stock of Anhui/1 possessed a mixture of amino acids at five positions, and the three amino acid changes in HA detected in the transmitted virus were detected in two of 39 HA clones representing the egg-grown virus stock of Anhui/1 (Supplementary Table 7). The selection of these mutations during A/Anhui replication and/or transmission in ferrets strongly suggests that these mutations have a biological role, possibly in HA stability and/or receptor-binding specificity or affinity. In fact, positions 131 and 135 are located near the receptor-binding pocket (Fig. 3). At position 71, both threonine and isoleucine are commonly found among H7 HAs, and the location of this position 'underneath' the receptor-binding pocket suggests a possible effect on HA stability (Fig. 3).

Our data indicate that Anhui/1 efficiently infects mammalian cells. We speculated that amino acid changes in Anhui/1 HA contribute to this host tropism. The HA-226L residue found in Anhui/1 is known to increase the affinity of H3 HAs (which are phylogenetically closely related to H7 HAs) to sialic acids linked to galactose by an α2,6-linkage ('human-type' receptors)[6]; by contrast, avian influenza viruses preferentially bind to sialic acids linked to galactose by an α2,3-linkage ('avian-type' receptors). In addition, Anhui/1 HA deviates from the avian virus consensus sequence at positions 186 and 189, which influence the receptor-binding preferences of H5 and H9 HAs, respectively[19–21].

To analyse receptor-binding preference, we subjected recombinant viruses possessing the Anhui/1, Shanghai/1 or Hangzhou/1 HA genes (see Supplementary Table 8) in combination with Anhui/1 NA genes and the remaining genes from A/Puerto Rico/8/34 (H1N1) (a laboratory-adapted strain) to glycan array analysis. All three viruses bound to α2,6-linked sialosides, unlike a representative avian virus (A/Vietnam/1203/2004 (H5N1); Vietnam/1203), which showed typical specificity for α2,3-linked sialosides (Fig. 3 and Supplementary Table 9). Anhui/1 and Hangzhou/1 HAs bound most strongly to α2,6-linked sialosides, and in particular to extended *N*-linked glycans that are found on human

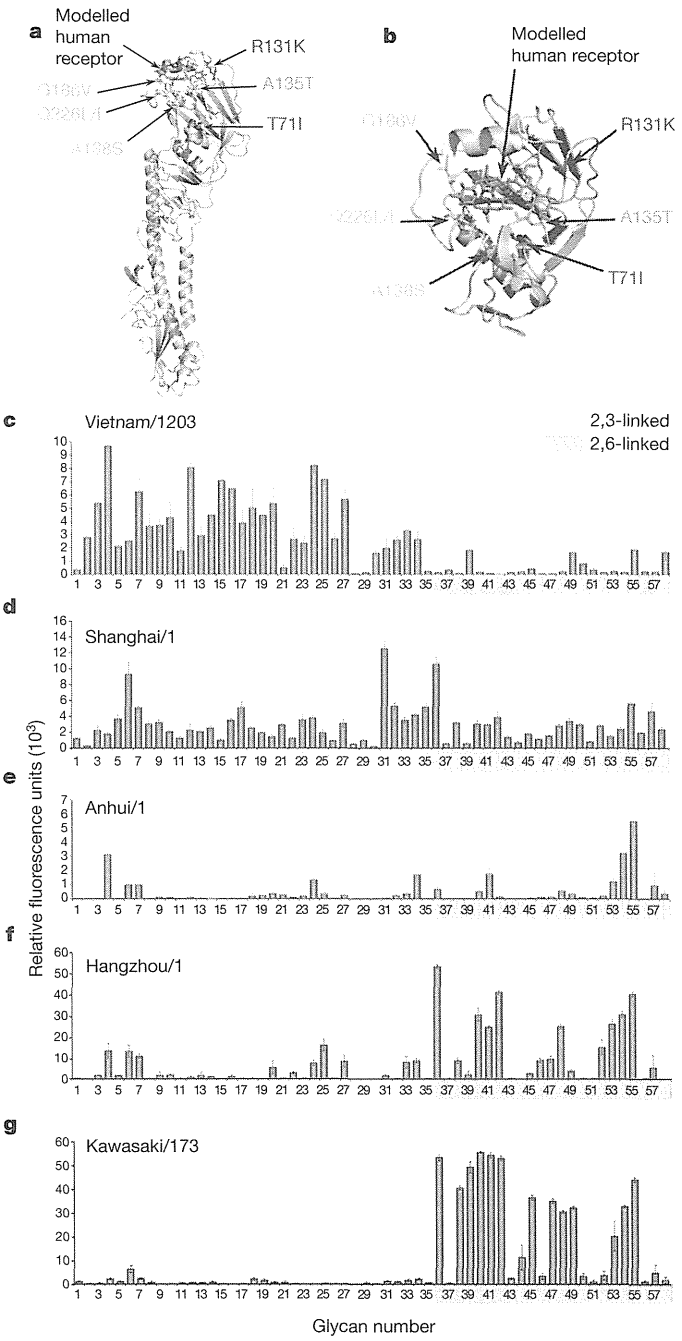

Figure 3 | HA structural analysis and glycan microarray analysis. **a**, Localization of amino acid changes in a virus from a ferret infected via respiratory droplets. Shown is the three-dimensional structure of A/Netherlands/219/2003 (H7N7) HA (Protein data bank (PDB) code, 4DJ6) in complex with human receptor analogues. **b**, Close-up view of the globular head. Mutations that increase affinity to human-type receptors are shown in cyan. Mutations that emerged in Anhui/1 HA during replication and/or transmission in ferrets are shown in red (T71I), green (A135T) and blue (R131K). The human receptor analogue (derived from its complex with H9 HA (PDB, 1JSI); shown in orange) is docked into the structure. Images were created with MacPymol (http://www.pymol.org/). **c–g**, Receptor specificities of recombinant viruses possessing A(H7N9) HAs (Anhui/1, Shanghai/1, Hangzhou/1) were compared with representative avian (A/Vietnam/1203/2004 (H5N1); Vietnam/1203) and human (A/Kawasaki/173/2001 (H1N1); Kawasaki/173) isolates in a glycan microarray containing α2,3 and α2,6 sialosides. Error bars represent standard deviations calculated from six replicate spots of each glycan. A complete list of glycans is found in Supplementary Table 9.

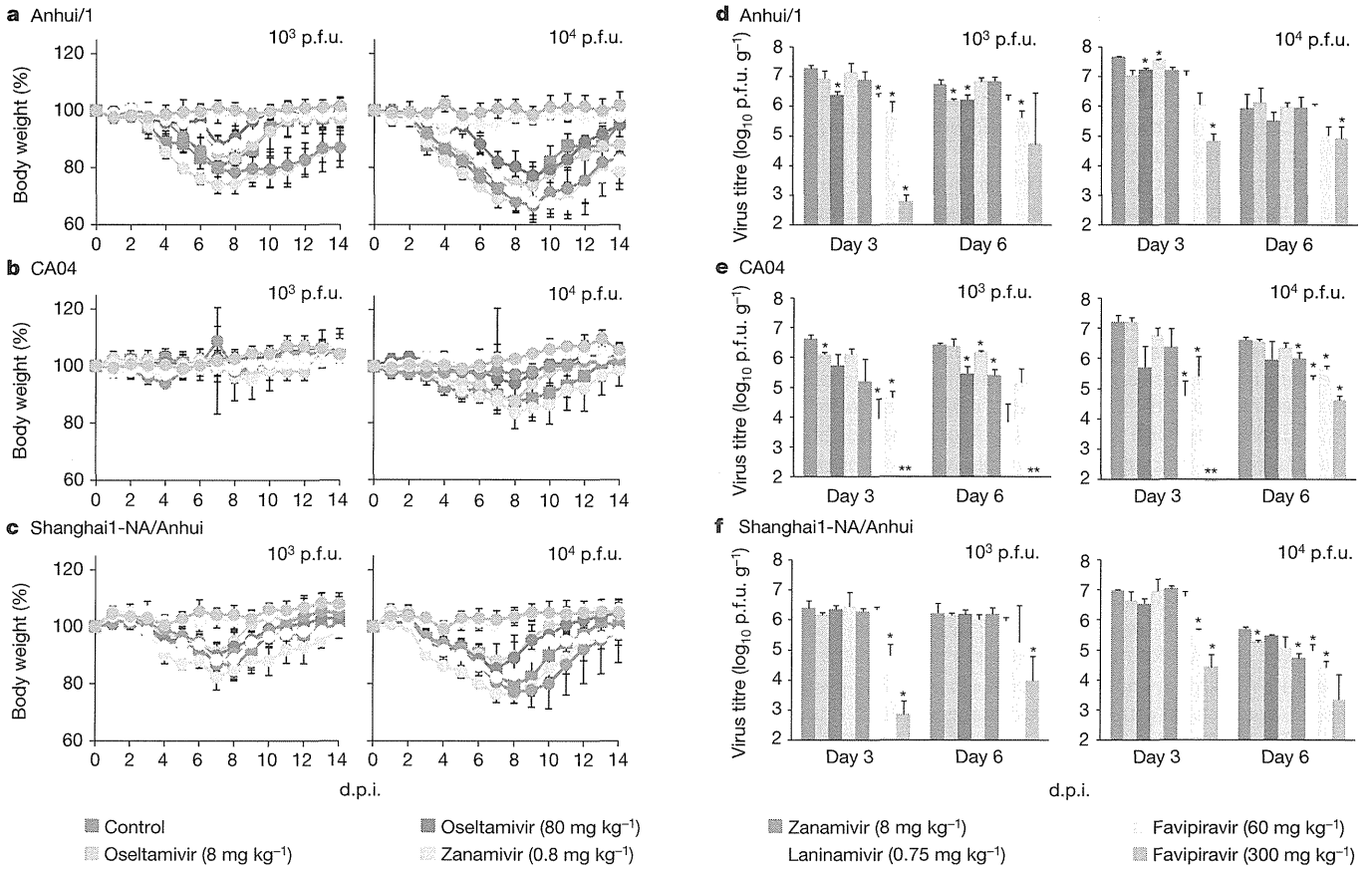

Figure 4 | Virus sensitivity to antivirals in mice. **a–f**, Mice were intranasally inoculated with 10^3 or 10^4 p.f.u. (50 µl) of Anhui/1 (**a**, **d**), CA04 (**b**, **e**) or recombinant Anhui/1 virus possessing Shanghai/1-NA-294K (**c**, **f**). At 2 h after infection, mice were treated with oseltamivir phosphate, zanamivir, laninamivir octanoate, favipiravir, or PBS and distilled water. PBS served as a control for intranasal administration; distilled water served as a control for oral administration. Body weights were monitored daily (**a–c**). Three mice per group were euthanized at 3 and 6 d.p.i., and the virus titres in lungs were determined by plaque assays in MDCK cells (**d–f**). Statistically significant differences between virus titres of control mice and those of mice treated with antiviral drugs were determined by using Welch's *t*-test or Student's *t*-test on the result of the F-test. The resulting *P* values were corrected by using Holm's method (*$P < 0.05$).**Virus was not recovered from all three animals infected with CA04 virus (for the 10^4 p.f.u. infection groups, the virus titres for the individual animals were $10^{2.0}$ p.f.u. ml^{-1} at 3 d.p.i. and $10^{2.2}$ and $10^{3.1}$ p.f.u. ml^{-1} at 6 d.p.i. For the 10^3 p.f.u. infection groups, the virus titres for the individual animals were $10^{2.2}$ and $10^{1.8}$ p.f.u. ml^{-1} at 3 d.p.i.). Error bars denote standard deviations.

bronchial epithelial cells[22] (Fig. 3). This binding pattern may be influenced by the 'human-type' residues at position 226 (Anhui/1 possesses HA-226L and Hangzhou/1 possesses HA-226I, the residues also found in human H3N2 influenza viruses at this position). Shanghai/1 HA (encoding the 'avian-type' HA-226Q) was less selective, binding equally well to both α2,6- and α2,3-linked sialosides (Fig. 3). The specificity of the recombinant Anhui/1 and Hangzhou/1 HA viruses was comparable to the 'human-type' receptor specificity of H5N1 virus receptor mutants that exhibit respiratory droplet transmission in ferrets[15,23], and to that of the human H7N3 A/New York/107/2003 isolate that exhibits contact, but not respiratory droplet transmission, in ferrets[24]. Notably, however, inhibition of the NA enzymatic function by inclusion of the neuraminidase inhibitor zanamivir in the glycan array analysis resulted in substantial increases in binding to α2,3-linked sialosides (as shown for Hangzhou/1 in Supplementary Fig. 10). Moreover, preliminary analysis of the specificity of the recombinant Anhui/1 H7 HA revealed preferential binding to α2,3 sialosides (R.P.d.V., R.M. & J.C.P., unpublished observations). Thus, the 'human-type' receptor specificity of A(H7N9) viruses assessed by glycan array seems to reflect the combined activities of HA and NA.

In pigs, we observed a mild infection with no clinical symptoms (Supplementary Tables 10 and 11, Supplementary Fig. 11 and Supplementary Information). Signs of disease were also absent in infected chickens and quails, which supported virus replication in a limited number of organs (a characteristic of low pathogenic avian influenza viruses) (Supplementary Tables 12–15 and Supplementary Information).

Antiviral compounds are currently the only therapeutic and prophylactic option for A(H7N9) infections. We therefore determined the *in vitro* 50% inhibitory concentration (IC_{50}) of several NA inhibitors (oseltamivir, zanamivir, laninamivir and peramivir), and of an experimental inhibitor of the viral RNA polymerase (favipiravir, also known as T-705) against egg-grown virus stocks of Anhui/1 and Shanghai/1. Sanger sequencing of the Shanghai/1 NA gene revealed the R294K mutation known to confer resistance to NA inhibitors for N2 and N9 NAs[25]. Both Anhui/1 and Shanghai/1 were sensitive to all NA inhibitors tested (Supplementary Table 16), consistent with a recent report that Shanghai/1 is susceptible to oseltamivir and zanamivir[26], but inconsistent with the presence of the R294K mutation. A possible explanation for this discrepancy is that the Shanghai/1 isolate contained a mixture of drug-sensitive and -resistant NA genes in which the drug-resistant subpopulation may not have been detected, as described in ref. 27. In fact, plaque purification of the egg-grown Shanghai/1 virus stock revealed a mixed population of NA genes encoding NA-294R or -294K. Testing of these variants confirmed that Shanghai/1-NA-294R was susceptible to NA inhibitors, whereas the NA-294K variant was not (Supplementary Table 16). Further testing demonstrated that 30% of oseltamivir-sensitive virus in the mixture is sufficient for results to be consistent with a purely sensitive virus population (Supplementary Table 17). The IC_{50} values of favipiravir, determined by plaque-reduction assays in MDCK cells, were low for Anhui/1 and the control CA04 virus (1.4 µg ml^{-1} and 1.2 µg ml^{-1},

respectively), suggesting that this compound could be a treatment option against A(H7N9) viruses resistant to NA inhibitors.

We also evaluated the therapeutic efficacy of the anti-influenza drugs in mice infected with Anhui/1, CA04 or a recombinant virus possessing the Shanghai/1 NA gene (encoding NA-294K) with the remaining genes from Anhui/1. Peramivir, which is structurally similar to oseltamivir but is administered intravenously, was omitted from these experiments. Mice infected with 10^3 and 10^4 p.f.u. of viruses were treated with the drugs beginning at 2 h post-infection. Some NA inhibitors had modest effects on the body-weight loss of Anhui/1-infected mice (Fig. 4a–c), consistent with limited, although statistically significant, effects on virus titre reduction (Fig. 4d–f). We currently do not know whether neuraminidase-resistant variants arose during Anhui/1 replication in mice, which may have limited virus susceptibility to NA inhibitors. In this context, it is interesting to note the poor efficacy of oseltamivir when used to treat a person infected with A(H7N9)[28], presumably owing to the emergence of drug-resistant variants. By contrast, favipiravir, which targets the viral polymerase complex, showed clear therapeutic effectiveness against both viruses at both doses tested.

In summary, on the basis of their sequences and phylogenetic relationships, Anhui/1 and Shanghai/1 originated from an avian host but possess several characteristic features of human influenza viruses, such as efficient binding to human-type receptors, efficient replication in mammalian cells (probably conferred by PB2-627K) and respiratory droplet transmission in ferrets (Anhui/1). These properties, together with the low efficacy of NA inhibitors and the lack of human immunity (we tested 500 human sera collected from various age groups in Japan and found no antibodies that recognized Anhui/1), make A(H7N9) viruses a formidable threat to public health.

METHODS SUMMARY

Viruses. A(H7N9) viruses were propagated in embryonated chicken eggs to produce viral stocks. Control viruses were propagated as described in Methods. All experiments with A(H7N9) viruses were carried out in approved biosafety level (BSL3) containment laboratories.

Animals. All animals were used according to approved protocols for their care and use. Detailed procedures are provided in Methods.

Antiviral sensitivity of viruses in mice. Six-week-old female BALB/c mice (Japan SLC; groups of six) were intranasally inoculated with 10^3 or 10^4 p.f.u. of Anhui/1, CA04 or a recombinant virus possessing the Shanghai/1 NA gene encoding NA-294K and the remaining genes from Anhui/1. At 2 h post-infection, mice were administered antiviral compounds as described in detail in Methods. Three mice per group were euthanized at 3 or 6 d.p.i. and the virus titres in lungs were determined by plaque assays in MDCK cells.

Full Methods and any associated references are available in the online version of the paper.

Received 23 May; accepted 20 June 2013.
Published online 10 July 2013.

1. World Health Organization. China–WHO Joint Mission on Human Infection with Avian Influenza A(H7N9) Virus. 18–24 April 2013, Mission Report. http://www.who.int/influenza/human_animal_interface/influenza_h7n9/ChinaH7N9JointMissionReport2013.pdf (2013).
2. Gao, R. *et al.* Human infection with a novel avian-origin influenza A (H7N9) virus. *N. Engl. J. Med.* **368,** 1888–1897 (2013).
3. World Health Organization. Number of confirmed human cases of avian influenza A(H7N9) reported to WHO. Report 8 – data in WHO/HQ as of 30 May 2013, 15:45 GMT+1. http://www.who.int/influenza/human_animal_interface/influenza_h7n9/08_ReportWebH7N9Number.pdf (2013).
4. Kageyama, T. *et al.* Genetic analysis of novel avian A(H7N9) influenza viruses isolated from patients in China, February to April 2013. *Euro Surveill.* **18,** 20453 (2013).
5. Liu, Q. *et al.* Genomic signature and protein sequence analysis of a novel influenza A (H7N9) virus that causes an outbreak in humans in China. *Microbes Infect.,* (2013).
6. Rogers, G. N. *et al.* Single amino acid substitutions in influenza haemagglutinin change receptor binding specificity. *Nature* **304,** 76–78 (1983).
7. Hatta, M., Gao, P., Halfmann, P. & Kawaoka, Y. Molecular basis for high virulence of Hong Kong H5N1 influenza A viruses. *Science* **293,** 1840–1842 (2001).
8. Subbarao, E. K., Kawaoka, Y. & Murphy, B. R. Rescue of an influenza A virus wild-type PB2 gene and a mutant derivative bearing a site-specific temperature-sensitive and attenuating mutation. *J. Virol.* **67,** 7223–7228 (1993).
9. Li, Z. *et al.* Molecular basis of replication of duck H5N1 influenza viruses in a mammalian mouse model. *J. Virol.* **79,** 12058–12064 (2005).
10. Itoh, Y. *et al.* In vitro and in vivo characterization of new swine-origin H1N1 influenza viruses. *Nature* **460,** 1021–1025 (2009).
11. van den Brand, J. M. *et al.* Severity of pneumonia due to new H1N1 influenza virus in ferrets is intermediate between that due to seasonal H1N1 virus and highly pathogenic avian influenza H5N1 virus. *J. Infect. Dis.* **201,** 993–999 (2010).
12. Min, J. Y. *et al.* Classical swine H1N1 influenza viruses confer cross protection from swine-origin 2009 pandemic H1N1 influenza virus infection in mice and ferrets. *Virology* **408,** 128–133 (2010).
13. Maines, T. R. *et al.* Transmission and pathogenesis of swine-origin 2009 A(H1N1) influenza viruses in ferrets and mice. *Science* **325,** 484–487 (2009).
14. Munster, V. J. *et al.* Pathogenesis and transmission of swine-origin 2009 A(H1N1) influenza virus in ferrets. *Science* **325,** 481–483 (2009).
15. Imai, M. *et al.* Experimental adaptation of an influenza H5 HA confers respiratory droplet transmission to a reassortant H5 HA/H1N1 virus in ferrets. *Nature* **486,** 420–428 (2012).
16. Jackson, S. *et al.* Reassortment between avian H5N1 and human H3N2 influenza viruses in ferrets: a public health risk assessment. *J. Virol.* **83,** 8131–8140 (2009).
17. Maines, T. R. *et al.* Lack of transmission of H5N1 avian-human reassortant influenza viruses in a ferret model. *Proc. Natl Acad. Sci. USA* **103,** 12121–12126 (2006).
18. Herfst, S. *et al.* Airborne transmission of influenza A/H5N1 virus between ferrets. *Science* **336,** 1534–1541 (2012).
19. Yamada, S. *et al.* Haemagglutinin mutations responsible for the binding of H5N1 influenza A viruses to human-type receptors. *Nature* **444,** 378–382 (2006).
20. Chutinimitkul, S. *et al. In vitro* assessment of attachment pattern and replication efficiency of H5N1 influenza A viruses with altered receptor specificity. *J. Virol.* **84,** 6825–6833 (2010).
21. Srinivasan, K., Raman, R., Jayaraman, A., Viswanathan, K. & Sasisekharan, R. Quantitative characterization of glycan-receptor binding of H9N2 influenza A virus hemagglutinin. *PLoS ONE* **8,** e59550 (2013).
22. Chandrasekaran, A. *et al.* Glycan topology determines human adaptation of avian H5N1 virus hemagglutinin. *Nature Biotechnol.* **26,** 107–113 (2008).
23. Chen, L. M. *et al. In vitro* evolution of H5N1 avian influenza virus toward human-type receptor specificity. *Virology* **422,** 103–113 (2012).
24. Belser, J. A. *et al.* Contemporary North American influenza H7 viruses possess human receptor specificity: implications for virus transmissibility. *Proc. Natl Acad. Sci. USA* **105,** 7558–7563 (2008).
25. McKimm-Breschkin, J. L. *et al.* Mutations in a conserved residue in the influenza virus neuraminidase active site decreases sensitivity to Neu5Ac2en-derived inhibitors. *J. Virol.* **72,** 2456–2462 (1998).
26. Centers for Disease Control & Prevention. Emergence of avian influenza A(H7N9) virus causing severe human illness - China, February–April 2013. *MMWR Morb. Mortal. Wkly Rep.* **62,** 366–371 (2013).
27. Wetherall, N. T. *et al.* Evaluation of neuraminidase enzyme assays using different substrates to measure susceptibility of influenza virus clinical isolates to neuraminidase inhibitors: report of the neuraminidase inhibitor susceptibility network. *J. Clin. Microbiol.* **41,** 742–750 (2003).
28. Liu, X. *et al.* Poor responses to oseltamivir treatment in a patient with influenza A (H7N9) virus infection. *Emerg. Microbes & Infections* **2,** e27 (2013).

Supplementary Information is available in the online version of the paper.

Acknowledgements We thank Y. Shu for A/Anhui/1/2013 (H7N9) and A/Shanghai/1/2013 (H7N9) viruses. We thank the IMSUT serum bank for providing human sera. We thank R. Webster for providing monoclonal antibody to A/seal/Massachusetts/1/80 (H7N7). Polyclonal anti-influenza virus H7 HA, A/Netherlands/219/2003 (H7N7) (anti-serum, goat) NR-9226, was obtained through the National Institutes of Health (NIH) Biodefense and Emerging Infections Research Resources Repository, National Institute of Allergy and Infectious Diseases (NIAID), NIH. We thank S. Watson for editing the manuscript, T. Suzuki, K. Takahashi, S. Fujisaki and H. Xu for discussions, and Y. Sato, H. Sugawara, A. Sato, M. Ejima and T. Miura for technical assistance. We thank Toyama Chemical Co. for providing favipiravir, Daiichi Sankyo Co. for providing laninamivir, F. Hoffmann-La Roche for providing oseltamivir carboxylate, GlaxoSmithKline for providing zanamivir and Shionogi & Co. for providing peramivir. This work was supported by the Japan Initiative for Global Research Network on Infectious Diseases from the Ministry of Education, Culture, Sports, Science and Technology, Japan; by grants-in-aid from the Ministry of Health, Labour and Welfare, Japan; by ERATO (Japan Science and Technology Agency); by NIAID Public Health Service research grants AI099274 and AI058113 to J.C.P., and by an NIAID-funded Center for Research on Influenza Pathogenesis (CRIP, HHSN266200700010C) to Y.K.

Author Contributions T.W., M.K., S. Fukuyama, M. Imai, S. Yamada, S.M., S. Yamayoshi, K.I.-H., Y. Sakoda, E.T., M.H., S.W., E.A.M., G.N., H.K., T.O., J.C.P., M.T. and Y.K. designed the study; T.W., M.K., S. Fukuyama, N.N., M. Imai, S. Yamada, S.M., S. Yamayoshi, K.I.-H., Y. Sakoda, E.T., R.M., T.N., M.H., H.I., D.Z., N.K., M.S., R.P.d.V., S.S., M. Okamatsu., T.T., Y.T., N.F., K.G., H.K., I.I., M. Ito, Y.S.-T., Y. Sugita, R.U., R.Y., A.J.E., G.Z., S. Fang, J.P., A.H., Y.U., T.S. and H.H. performed the experiments; T.W., M.K., S. Fang, N.N., M. Imai, S. Yamayoshi, S.M., S. Yamada, K.I.-H., Y. Sakoda, E.T., R.M., T.N., M.H., H.I., D.Z., R.P.V., S.S., T.T., Y.T., H.K., E.K. and H. H. analysed the data; T.W., S. Fukuyama, N.N., E.T., R.M., M.H., R.P.d.V., M. Ozawa, G.N., T.O., J.C.P., H.H., M.T. and Y.K. wrote the manuscript; Y.K. oversaw the project. T.W., M.K., S. Fukuyama, N.N. and M. Imai contributed equally to this work.

Author Information Reprints and permissions information is available at www.nature.com/reprints. The authors declare competing financial interests: details are available in the online version of the paper. Readers are welcome to comment on the online version of the paper. Correspondence and requests for materials should be addressed to Y.K. (kawaokay@svm.vetmed.wisc.edu).

METHODS

Viruses. Anhui/1 and Shanghai/1, both kindly provided by Y. Shu, and Dk/GM466 were propagated in embryonated chicken eggs. For antigenic characterization by haemagglutination inhibition assays (see below for detailed procedures), Anhui/1 was also propagated in MDCK cells. CA04, Kawasaki/173 and Vietnam/1203 were propagated in MDCK cells. All experiments with H7N9 viruses were performed in enhanced biosafety level 3 (BSL3) containment laboratories at the University of Tokyo and the National Institute of Infectious Diseases, Japan, which are approved for such use by the Ministry of Agriculture, Forestry and Fisheries, Japan; or in enhanced BSL3 containment laboratories at the University of Wisconsin-Madison, which are approved for such use by the Centers for Disease Control and Prevention and by the US Department of Agriculture.

Cells. MDCK cells were maintained in Eagle's MEM containing 5% newborn calf serum. Human embryonic kidney 293T cells were maintained in DMEM containing 10% FCS. Normal human bronchial epithelial cells (NHBEs) were obtained from Lonza. The monolayers of NHBE cells were cultured and differentiated as previously described[29]. All cells were incubated at 37 °C with 5% CO_2.

Antiviral compounds. Laninamivir and laninamivir octanoate were kindly provided by Daiichi Sankyo Co. Favipiravir was kindly provided by Toyama Chemical Co. and oseltamivir carboxylate was provided by F. Hoffmann-La Roche. Zanamivir was kindly provided by GlaxoSmithKline. Peramivir was kindly provided by Shionogi & Co.

Reverse genetics. Plasmid-based reverse genetics for influenza virus generation was performed as previously described[30]. In brief, plasmids encoding the complementary DNAs for the eight viral RNA segments under the control of the human RNA polymerase I promoter and the mouse RNA polymerase I terminator (referred to as PolI plasmids), and plasmids for the expression of the viral PB2, PB1, PA and nucleoprotein proteins derived from a laboratory-adapted influenza A virus strain A/WSN/33 (H1N1), under the control of the chicken β-actin promoter[31], were transfected into 293T cells with the help of a transfection reagent, Trans-IT 293 (Mirus). At 48 h post-transfection, culture supernatants were collected and inoculated to embryonated chicken eggs for virus propagation.

Growth kinetics of virus in cell culture. MDCK cells were infected in triplicate in 12-well plates with Anhui/1, Dk/GM466 or CA04 at a multiplicity of infection (m.o.i.) of 0.01. After incubation at 37 °C for 1 h, the viral inoculum was replaced with MEM containing 0.3% bovine serum albumin (with 0.75 μg ml^{-1} trypsin treated with L-1-tosylamide-2- phenylethyl chloromethyl ketone), followed by further incubation at 37 °C. Culture supernatants collected at the indicated time points were subjected to virus titration by using plaque assays in MDCK cells.

Cultures of differentiated NHBE cells grown on semipermeable membrane supports were washed extensively with DMEM to remove accumulated mucus and infected in triplicate with virus at a m.o.i. of 0.001 from the apical surface. The inoculum was removed after 30 min of incubation at 33 °C or 37 °C, and cells were further incubated at 33 °C or 37 °C. Samples were collected at 6, 12, 24, 48, 72 and 96 h post-infection from the apical surface. Apical collection was performed by adding 500 μl of medium to the apical surface, followed by incubation for 30 min at 33 °C or 37 °C, and removal of the medium from the apical surface. The titres of viruses released into the cell culture supernatant were determined by plaque assay in MDCK cells.

Animal experiments. The sample sizes ($n = 3$) for the mouse, ferret, quail and chicken studies were chosen because they have previously been shown to be sufficient to evaluate a significant difference among groups[10,14,32–34]. For the non-human primate and pig experiments, two or three animals per group were used and no statistical analysis was performed. No method of randomization was used to determine how animals were allocated to the experimental groups and processed in this study. The investigator was not blinded to the group allocation during the experiments or when assessing the outcome.

Experimental infection of mice. Six-week-old female BALB/c mice (Japan SLC) were used in this study. Baseline body weights were measured before infection. Under anaesthesia, four mice per group were intranasally inoculated with 10^1, 10^2, 10^3, 10^4, 10^5 or 10^6 p.f.u. (50 μl) of Anhui/1, Shanghai/1, Dk/GM466 or CA04. Body weight and survival were monitored daily for 14 days. For virological and pathological examinations, six mice per group were intranasally infected with 10^4 or 10^6 p.f.u. (50 μl) of the viruses and three mice per group were euthanized at 3 and 6 d.p.i. The virus titres in various organs were determined by plaque assays in MDCK cells. All experiments with mice were performed in accordance with the University of Tokyo's Regulations for Animal Care and Use and approved by the Animal Experiment Committee of the Institute of Medical Science, the University of Tokyo.

Experimental infection of ferrets. Five- to eight-month-old female ferrets (Triple F Farms), which were serologically negative by haemagglutination inhibition assay for currently circulating human influenza viruses, were used in this study. Under anaesthesia, six ferrets per group were intranasally inoculated with 10^6 p.f.u. (0.5 ml) of Anhui/1, Shanghai/1, Dk/GM466 or CA04. Three ferrets per group were euthanized at 3 and 6 d.p.i. for virological and pathological examinations. The virus titres in various organs were determined by plaque assays in MDCK cells. All experiments with ferrets were performed in accordance with the University of Tokyo's Regulations for Animal Care and Use and approved by the Animal Experiment Committee of the Institute of Medical Science, the University of Tokyo.

Ferret transmission study. Pairs of ferrets were individually housed in adjacent wireframe cages that prevented direct and indirect contact between animals but allowed spread of influenza virus by respiratory droplets. Under anaesthesia, three ferrets per group were intranasally inoculated with 0.5 ml of 10^6 p.f.u. ml^{-1} of Anhui/1, Dk/GM466 or CA04 (inoculated ferrets). One day after infection, three naive ferrets (contact ferrets) were each placed in a cage adjacent to an infected ferret (in these cages, infected and contact ferrets are separated by ~5 cm). Body weight and temperature were monitored every other day. Nasal washes were collected from infected ferrets on day 1 after inoculation and from contact ferrets on day 1 after co-housing, and then every other day (for up to 9 days) for virological examinations. The virus titres in nasal washes were determined by plaque assays in MDCK cells.

Experimental infection of cynomolgus macaques. Approximately 2-year-old male cynomolgus macaques (*Macaca fascicularis*) from Cambodia (obtained from Japan Laboratory Animals), weighing 2.2–2.8 kg and serologically negative by AniGen AIV antibody ELISA, which detects infection of all influenza A virus subtypes (Animal Genetics) and neutralization against A/Osaka/1365/2009 (H1N1pdm09), A/Kawasaki/UTK-4/2009 (seasonal H1N1), A/Kawasaki/UTK-20/2008 (H3N2), B/Tokyo/UT-E2/2008 (type B) and A/duck/Hong Kong/301/78 (H7N2) viruses, were used in this study. Under anaesthesia, six and four macaques were inoculated with Anhui/1 or Dk/GM466 (10^7 p.f.u. ml^{-1} each), respectively, through a combination of intratracheal (4.5 ml), intranasal (0.5 ml per nostril), ocular (0.1 ml per eye) and oral (1 ml) routes (resulting in a total infectious dose of 6.7×10^7 p.f.u.). Body temperature was monitored at 0, 1, 3, 5 and 6 d.p.i. by rectal thermometer. Nasal and tracheal swabs were collected at 1, 3, 5 and 6 d.p.i. for virological examinations. Three Anhui/1- and two Dk/GM466-infected macaques per group were euthanized at 3 and 6 d.p.i. for virological and pathological examinations. Virus titres were determined by plaque assays in MDCK cells. All experiments with macaques were performed in accordance with the Regulation on Animal Experimentation Guidelines at Kyoto University (5 February, 2007) and were approved by the Committee for Experimental Use of Nonhuman Primates in the Institute for Virus Research, Kyoto University.

Experimental infection of miniature pigs. Two- to three-month-old female specific-pathogen-free miniature pigs (NIBS line; Nippon Institute for Biological Science), which were serologically negative by neutralization assay for currently circulating human and swine influenza viruses, were used in this study. Baseline body temperatures were measured before infection. Four and two pigs were intranasally inoculated with 10^7 p.f.u. (1 ml) of Anhui/1 or Dk/GM466, respectively. Body temperature was monitored daily. Nasal swabs were collected every day for virological examinations. Two pigs per group were euthanized at 3 d.p.i. for virological and pathological examinations; the remaining two Anhui/1-inoculated pigs were euthanized at 6 d.p.i. Virus titres were determined by plaque assays in MDCK cells. All experiments with miniature pigs were performed in accordance with guidelines established by the Animal Experiment Committee of the Graduate School of Veterinary Medicine, Hokkaido University, and were approved by the Institutional Animal Care and Use Committee of Hokkaido University.

Experimental infection of chickens. Four-week-old female specific-pathogen-free chickens (Nisseiken Co.) were used in this study. Six chickens per group were intranasally inoculated with 2×10^6 p.f.u. (0.2 ml) of Anhui/1 or Dk/GM466. Tracheal and cloacal swabs were collected every day for virological examinations. Three chickens per group were euthanized at 3 and 6 d.p.i. for virological examinations. The virus titres in various organs and swabs were determined by plaque assays in MDCK cells. All experiments with chickens were performed in accordance with the Animal Experimentation Guidelines of the National Institute of Infectious Disease (NIID) and were approved by the Animal Care and Use Committee of the NIID.

Experimental infection of quails. Four-month-old female quails (Yamanaka Koucho En) were used in this study. Six quails per group were intranasally inoculated with 2×10^6 p.f.u. (0.2 ml) of Anhui/1 or Dk/GM466. Tracheal and cloacal swabs were collected every day for virological examinations. Three quails per group were euthanized at 3 and 6 d.p.i. for virological examinations. The virus titres in various organs and swabs were determined by plaque assays in MDCK cells. All experiments with quails were performed in accordance with the University of Tokyo's Regulations for Animal Care and Use and were approved by the Animal Experiment Committee of the Institute of Medical Science, the University of Tokyo.

Pathological examination. Excised tissues of animal organs preserved in 10% phosphate-buffered formalin were processed for paraffin embedding and cut into 3-μm-thick sections. One section from each tissue sample was stained using a standard haematoxylin and eosin procedure, whereas another one was processed for immunohistological staining with a rabbit polyclonal antibody for type A influenza nucleoprotein antigen (prepared in our laboratory) that reacts comparably with all of the viruses tested in this study. Specific antigen–antibody reactions were visualized with 3,3′-diaminobenzidine tetrahydrochloride staining by using the DAKO LSAB2 system (DAKO Cytomation).

Cytokine and chemokine measurement. Macaque lung homogenates and serum samples were processed with the MILLIPLEX MAP Non-human Primate Cytokine/Chemokine Panel–Premixed 23-Plex (Merck Millipore). Array analysis was performed by using the Bio-Plex Protein Array system (Bio-Rad Laboratories).

NA inhibition assay. *In vitro* NA activity of viruses was determined by using the commercially available NA-Fluor Influenza Neuraminidase Assay Kit (Applied Biosystems). In brief, diluted viruses were mixed with the indicated amounts of oseltamivir carboxylate, zanamivir, laninamivir or peramivir and incubated at 37 °C for 30 min. Methylumbelliferyl-*N*-acetylneuraminic acid (MUNANA) was then added as a fluorescent substrate, and the mixture was incubated at 37 °C for 1 h. The reaction was stopped by adding 0.12 M Na_2CO_3 in 40% ethanol. The fluorescence of the solution was measured at an excitation wavelength of 355 nm and an emission wavelength of 460 nm, and the IC_{50} values were calculated.

Polymerase inhibitor sensitivity assay. 8×10^5 MDCK cells were infected with approximately 50 p.f.u. of viruses. After incubation at 37 °C for 1 h, the viral inoculum was replaced with agarose medium containing various concentrations of favipiravir. After the cells were incubated at 37 °C for 2 days, plaques were visualized by crystal violet staining and counted.

Antiviral sensitivity of viruses in mice. Under anaesthesia, six mice per group were intranasally inoculated with 10^3 or 10^4 p.f.u. (50 μl) of Anhui/1, CA04 or a recombinant virus possessing the Shanghai/1 NA gene encoding NA-294K and the remaining genes from Anhui/1. At 2 h after inoculation, mice were treated with the following antiviral compounds: (1) oseltamivir phosphate: 4 or 40 mg per kg per 200 μl, administered orally twice a day for 5 days; (2) zanamivir: 0.8 or 8 mg per kg per 50 μl, administered intranasally once daily for 5 days; (3) laninamivir: 0.75 mg per kg per 50 μl, administered intranasally once during the entire experimental course; (4) favipiravir: 30 or 150 mg per kg per 200 μl, administered orally twice a day for 5 days; (5) or PBS intranasally (50 μl) and distilled water orally administered. For virological examinations, three mice per group were euthanized at 3 and 6 d.p.i. The virus titres in lungs were determined by plaque assays in MDCK cells.

Antigenicity characterization by HI assays. Anti-H7 HA monoclonal antibodies 46/6, 46/2 and 55/3 against A/seal/Massachusetts/1/80 (H7N7) virus were kindly provided by R. G. Webster. The goat polyclonal antibody NR-9226 (raised against A/Netherlands/219/2003 (H7N7)) was obtained from BEI Resources. The remaining antibodies, that is, mouse monoclonal antibodies B1275m and B1275m (raised against A/Netherlands/219/2003 (H7N7), MyBioSource), 127-10023 (raised against A/FPV/Rostock/34 (H7N1), RayBiotech), 10H9, 9A9 and 1H11 (raised against A/FPV/Rostock/34 (H7N1), HyTest), and rabbit polyclonal antibody MBS432028 (raised against A/chicken/MD/MINHMA/2004 (H7N2), MyBioSource) were commercially available. Anhui/1 propagated in embryonated chicken eggs or in MDCK cells was used in this study. Antibodies were serially diluted twofold with PBS in 96-well U-bottom microtitre plates and mixed with the amount of virus equivalent to eight haemagglutination units, followed by incubation at room temperature (25 °C) for 30 min. After adding 50 μl of 0.5% turkey red blood cells, the mixtures were gently mixed and incubated at room temperature for a further 45 min. haemagglutination inhibition titres are expressed as the inverse of the highest antibody dilution that inhibited haemagglutination (Supplementary Table 18). These data were used to select antibodies for glycan arrays.

Serology with human sera. Human sera, collected in Japan in November 2012 from 200 donors ranging in age from 20 to 63 years, were treated with receptor-destroying enzyme (Denka Seiken Co). Twofold serial dilutions of the treated sera were mixed with 100 p.f.u. of Anhui/1 and incubated at 37 °C for 1 h. MDCK cells were inoculated with the virus-serum mixtures and cultured for 3 days. The neutralizing activity of the sera was determined based on the cytopathic effects in inoculated cells. All experiments with human sera were approved by the Research Ethics Review Committee of the Institute of Medical Science, the University of Tokyo (approval number: 21-38-1117).

A total of 300 serum samples were also obtained from the serum bank of the National Institute of Infectious Diseases in Japan. Samples were collected from different regions of Japan during 2010–2011. Subjects were divided into 10 age groups, 30 samples per group, and analysed for antibodies against Anhui/1 by use of the haemagglutination inhibition assay with 0.5% turkey red blood cells.

Glycan arrays. Glycan array analysis was performed on a glass slide microarray containing 6 replicates of 57 diverse sialic acid-containing glycans including terminal sequences and intact *N*-linked and *O*-linked glycans found on mammalian and avian glycoproteins and glycolipids[35]. β-propiolactone-inactivated viruses containing A(H7N9) virus HA and NA genes in the background of A/Puerto Rico/8/34 (H1N1) virus were applied to the array at dilutions of 128–512 haemagglutination units ml^{-1}. After incubation at room temperature for 1 h, slides were washed and overlaid with a 1:200 dilution of rabbit or goat anti-H7 antibody for 1 h (selected on the basis of antibody characterization with several H7 viruses; see Supplementary Table 18), and finally with anti-rabbit IgG Alexa Fluor 488 or anti-goat IgG Alexa Fluor 647 (Invitrogen) at 10 μg ml^{-1}. Slides were then washed and scanned on a ProScanArray Express HT (PerkinElmer) confocal slide scanner to detect bound virus. A complete list of glycans present on the array is provided in Supplementary Materials (Supplementary Table 9).

Electron microscopy. Anhui/1 was inoculated into 10-day-old embryonated chicken eggs and the allantoic membranes were collected 24 h after inoculation. They were then processed for ultrathin section electron microscopy and scanning electron microscopy as described previously[10,36].

Statistical analysis. All statistical analyses were performed using JMP Pro 9.0.2 (SAS Institute). Statistically significant differences between the virus titres of Dk/GM466-infected mice and those of other mice were determined by using Welch's *t*-test with Bonferroni's correction. Comparisons of virus titres in antiviral sensitivity assays in mice were also done using Welch's *t*-test or Student's *t*-test on the result of the F-test. The resulting *P* values were corrected by using the Holm's method.

Biosafety and biosecurity. All recombinant DNA protocols were approved by the University of Wisconsin-Madison's Institutional Biosafety Committee after risk assessments were conducted by the Office of Biological Safety, and by the University of Tokyo's Subcommittee on Living Modified Organisms, and, when required, by the competent minister of Japan. In addition, the University of Wisconsin-Madison Biosecurity Task Force regularly reviews the research program and ongoing activities of the laboratory. The task force has a diverse skill set and provides support in the areas of biosafety, facilities, compliance, security and health. Members of the Biosecurity Task Force are in frequent contact with the principal investigator and laboratory personnel to provide oversight and assure biosecurity. All experiments with H7N9 viruses were performed in enhanced BSL3 containment laboratories. Ferret transmission studies were conducted by two scientists with DVM and/or PhD degrees that each had more than 5 years of experience working with highly pathogenic influenza viruses and performing animal studies with such viruses. Our staff who work with ferrets, nonhuman primates, pigs, chickens and quails wear disposable overalls and powered air-purifying respirators that filter the air. Biosecurity monitoring of the facilities is ongoing. All personnel complete rigorous biosafety, BSL3 and Select Agent (for the US laboratory) training before participating in BSL3-level experiments. The principal investigator participates in training sessions and emphasizes compliance to maintain safe operations and a responsible research environment. The laboratory occupational health plans are in compliance with policies at the respective institutions (University of Wisconsin-Madison and the University of Tokyo Occupational Health Programs).

29. Jakiela, B., Brockman-Schneider, R., Amineva, S., Lee, W. M. & Gern, J. E. Basal cells of differentiated bronchial epithelium are more susceptible to rhinovirus infection. *Am. J. Respir. Cell Mol. Biol.* **38,** 517–523 (2008).
30. Neumann, G. *et al.* Generation of influenza A viruses entirely from cloned cDNAs. *Proc. Natl Acad. Sci. USA* **96,** 9345–9350 (1999).
31. Niwa, H., Yamamura, K. & Miyazaki, J. Efficient selection for high-expression transfectants with a novel eukaryotic vector. *Gene* **108,** 193–199 (1991).
32. Makarova, N. V., Ozaki, H., Kida, H., Webster, R. G. & Perez, D. R. Replication and transmission of influenza viruses in Japanese quail. *Virology* **310,** 8–15 (2003).
33. Liu, J. *et al.* Highly pathogenic H5N1 influenza virus infection in migratory birds. *Science* **309,** 1206 (2005).
34. Zhu, H. *et al.* Infectivity, transmission, and pathology of human H7N9 influenza in ferrets and pigs. *Science* http://dx.doi.org/10.1126/science.1239844 (2013).
35. Xu, R. *et al.* A recurring motif for antibody recognition of the receptor-binding site of influenza hemagglutinin. *Nature Struct. Mol. Biol.* **20,** 363–370 (2013).
36. Noda, T. *et al.* Architecture of ribonucleoprotein complexes in influenza A virus particles. *Nature* **439,** 490–492 (2006).

MODERN PATHOLOGY (2013) 26, 357–369

Pathological study of archival lung tissues from five fatal cases of avian H5N1 influenza in Vietnam

Noriko Nakajima[1], Ngo Van Tin[2], Yuko Sato[1], Hoang Ngoc Thach[2], Harutaka Katano[1], Pho Hong Diep[2], Toshio Kumasaka[3], Nguyen Trung Thuy[2], Hideki Hasegawa[1], Luong Thi San[4], Shoji Kawachi[5], Nguyen Thanh Liem[4], Kazuo Suzuki[6] and Tetsutaro Sata[1,7]

[1]*Department of Pathology, National Institute of Infectious Diseases, Tokyo, Japan;* [2]*Department of Anatomical Pathology, National Hospital of Pediatrics, Hanoi, Vietnam;* [3]*Department of Pathology, Japanese Red Cross Medical Center, Tokyo, Japan;* [4]*National Hospital of Pediatrics, Hanoi, Vietnam;* [5]*Surgical Operation Department, National Center for Global Health and Medicine, Tokyo, Japan;* [6]*Safety Control Department, University Hospital, School of Medicine, and General Medical Education Center, Teikyo University, Tokyo, Japan and* [7]*Toyama Institute of Health, Toyama, Japan*

Highly pathogenic avian H5N1 influenza virus (H5N1) infection in humans causes acute respiratory distress syndrome, leading to multiple organ failure. Five fatal cases of H5N1 infection in Vietnam were analyzed pathologically to reveal virus distribution, and local proinflammatory cytokine and chemokine expression profiles in formalin-fixed, paraffin-embedded lung tissues. Our main histopathological findings showed diffuse alveolar damage in the lungs. The infiltration of myeloperoxidase-positive and/or CD68 (clone KP-1)-positive neutrophils and monocytes/macrophages was remarkable in the alveolar septa and alveolar spaces. Immunohistochemistry revealed that H5N1 mainly infected alveolar epithelial cells and monocytes/macrophages in lungs. H5N1 replication was confirmed by detecting H5N1 mRNA in epithelial cells using *in situ* hybridization. Quantitation of H5N1 RNA using quantitative reverse transcription PCR assays revealed that the level of H5N1 RNA was increased in cases during early phases of the disease. We quantified the expression of tumor necrosis factor-alpha (TNF-α), interleukin (IL)-6, IL-8, regulated on activation normal T-cell expressed and secreted (commonly known as RANTES), and interferon-gamma-inducible protein of 10 kDa (IP-10) in formalin-fixed, paraffin-embedded lung sections. Their expression levels correlated with H5N1 RNA copy numbers detected in the same lung region. Double immunofluorescence staining revealed that TNF-α, IL-6, IL-8 and IP-10 were expressed in epithelial cells and/or monocytes/macrophages. In particular, IL-6 was also expressed in endothelial cells. The dissemination of H5N1 beyond respiratory organs was not confirmed in two cases examined in this study.
Modern Pathology (2013) **26,** 357–369; doi:10.1038/modpathol.2012.193; published online 23 November 2012

Keywords: autopsy; cytokine; chemokine; H5N1; influenza; immunohistochemistry; lung

Since the outbreak of highly pathogenic avian H5N1 influenza virus infection in humans in 2003, the WHO has reported 608 confirmed cases from 15 countries, with a mortality rate of about 60% by August 2012 (http://www.who.int/influenza/human_animal_interface/EN_GIP_20120810CumulativeNumberH5N1cases.pdf). The potential for mutation and reassortment of the viral genome, which may be responsible for human-to-human transmission, has increased the threat of an influenza pandemic.

Many H5N1-infected patients develop acute respiratory distress syndrome and die because of respiratory failure or multiple organ failure.[1,2] Pathological study of autopsied cases revealed that the H5N1 virus infected type I and type II pneumocytes and caused primary viral pneumonia, which further developed into acute respiratory distress syndrome.[3–18] Although seasonal influenza virus infection is also associated with pneumonia, the virus mainly infects epithelial cells of the upper respiratory tract.[19–21] Complications involving

Correspondence: Dr N Nakajima, MD, PhD, Department of Pathology, National Institute of Infectious Diseases, 1-23-1 Toyama, Shinjuku, Tokyo 162-8640, Japan.
E-mail: tenko@nih.go.jp
Received 22 June 2012; revised 20 September 2012; accepted 20 September 2012; published online 23 November 2012

pneumonia are often due to bacterial infection. In the case of the influenza pandemic that occurred in 2009, the virus, designated A(H1N1)pdm09, infected pneumocytes in some patients. It also caused severe respiratory failure, similar to that seen for H5N1 infection, during the first year of the outbreak.[22–26] The analysis of 20 autopsied A(H1N1)pdm09 infection cases in Japan revealed that diffuse alveolar damage, similar to that seen in a case of H5N1 infection, was present in the lungs of 5 cases (25%).[27]

The pathological study of human tissues can be restricted because of the difficulty in obtaining samples, but it is crucial for elucidating pathogenesis of the disease. There have been only 16 reports of pathological studies carried out on fatal cases of H5N1 infection. These have been reported from Hong Kong,[3–6] Thailand,[7–13] China[14–17] and Vietnam.[18] Lungs infected with H5N1 presented with diffuse alveolar damage in all cases. In most cases, H5N1 antigens and RNA were detected in extrapulmonary organs, suggesting disseminated systemic H5N1 infection and viremia.

Nearly 77% (10/13 patients) of H5N1 infection cases have resulted in death at the National Hospital of Pediatrics Hanoi, since December 2003. In this study, post-mortem biopsied or autopsied tissues from five fatal cases were analyzed pathologically to reveal virus distribution and the expression levels of cytokines and chemokines in lungs. Immunohistochemistry, *in situ* hybridization, double immunofluorescence staining and quantitative reverse transcription PCR (qRT-PCR) methods were used in our studies.

Materials and methods

Patients and Formalin-Fixed, Paraffin-Embedded Tissues

H5N1 infection of the five cases was confirmed by detecting viral RNA in bronchiolar aspirate using RT-PCR. The numbering of the case was in order of the shortness of the disease duration. In three cases (cases 1, 4 and 5; Table 1), post-mortem biopsied lung tissues were examined; these cases have been reported previously in a short communication.[18] In the other two cases, patients were autopsied at National Hospital of Pediatrics; in addition to lung tissue, liver, heart, kidney, intestine, spleen and pancreas were examined in case 2. For case 3, liver, heart and kidney tissue were also examined in addition to lung tissue (Table 1). Only formalin-fixed, paraffin-embedded tissues were available for this study. This study was approved by the institutional medical ethical committee of the National Institute of Infectious Diseases, Japan (approval no. 320) and National Hospital of Pediatrics Hanoi.

Histopathological Studies and Immunohistochemistry

The formalin-fixed, paraffin-embedded tissues were cut (3-μm thick sections) and mounted on silane-coated glass slides. Histopathological studies were performed on all samples using hematoxylin–eosin (HE) staining. For lung sections, Elastica–Masson Goldner staining was also done. Immunohistochemistry for influenza A nucleoprotein antigen (InfA-NP) was performed to evaluate the distribution of H5N1 antigens with a mouse monoclonal antibody against InfA-NP[28] as previously described.[18,23,27]

Immunohistochemistry for cell type-specific marker proteins, cytokines and chemokines was performed using primary antibodies against the following proteins: myeloperoxidase (MPO; Nichirei Bioscience, Tokyo, Japan); neutrophil elastase (DAKO Cytomation, Copenhagen, Denmark); CD68 (KP-1 or PGM-1; DAKO); CD8 (Novocastra Laboratories, Newcastle, UK); tumor necrosis factor-alpha (TNF-α; BD Pharmingen, San Diego, CA, USA); interleukin (IL)-6 (R&D Systems, Minneapolis, MN, USA); IL-8 (R&D Systems); regulated on activation normal T-cell expressed and secreted (RANTES; R&D Systems); and interferon-gamma-inducible protein of 10 kDa (IP-10; R&D Systems). After incubation with these primary antibodies, signals were detected using the avidin–biotin complex immunoperoxidase method (LSAB2, DAKO). A biotin-free catalyzed signal amplification system (CSAII, DAKO) was used for the detection of TNF-α, IL-6 and CD8. The EnVision system (DAKO) was used for the detection of neutrophil elastase. As a negative control, an irrelevant antibody was used in place of the primary antibody.

In Situ Hybridization

Influenza virus genomic RNA and mRNA were detected in formalin-fixed, paraffin-embedded lung sections by *in situ* hybridization AT tailing combined with a catalyzed signal amplification method (ISH-AT) as described previously.[29,30] Anti-sense and sense ISH-AT probes against H5N1 nucleoprotein (NP) genes were prepared and used to detect H5N1 mRNA and genomic RNA. The anti-sense ISH-AT probe against the rabies virus NP gene was used as an irrelevant negative control (Table 2).

Double Immunofluorescence Staining

Double immunofluorescence staining for InfA-NP, cytokines, chemokines or for cell type-specific marker proteins was performed. We used antibodies against the following marker proteins to determine cell type: MPO (DAKO); surfactant apoprotein D (SP-D; Chemicon, Temecula, CA, USA); CD68 (KP-1 or PGM-1; DAKO); cytokeratin AE1/AE3 (DAKO); epithelial membrane antigen (EMA; DAKO); and CD34 (Novocastra). AlexaFluor 488-conjugated anti-